

DATA REPOSITORY

Mineral separation

Standard density and magnetic separation techniques were used to extract apatite and zircon grains from granodiorite samples, and hornblende and high-quality groundmass grains from lavas.

U-Pb zircon dating methods

For zircon U-Pb analysis (Kosler and Sylvester, 2003), zircons from one sample from each transect were mounted in resin and polished. Data were produced on a New Wave Nd:YAG 213 nm laser ablation system, coupled to an Agilent 7500a quadrupole mass spectrometer. Real time data were processed using GLITTER v4.4 data reduction software (www.gitter-gemoc.com); isotope ratios and age estimates are shown in Tables DR1 and DR2, and U-Pb concordia in Fig. DR1. Repeated measurements of the zircon Plesovice standard (TIMS reference age 337.13 ± 0.37 Ma; Slama et al., 2008) and NIST 612 silicate glass (Pearce et al., 1997) were used to correct for instrumental mass bias and depth-dependent inter-element fractionation of Pb, Th and U. Age estimates were calculated using Isoplot v3.6 (Ludwig, 2008). Zircon U-Pb analysis was carried out at Birkbeck College, University of London, by C.M. under the supervision of A.C.

Apatite fission track dating methods

For apatite fission track (AFT) analysis, spontaneous tracks in apatite were revealed using 5M HNO₃ at 20 °C for 20 seconds. Etched grain mounts were packed with mica external detectors and corning glass dosimeters (CN5) and irradiated in the FRM 11 thermal neutron facility at the University of Munich. Ages (Table DR3) were determined using the zeta calibration method and IUGS recommended age standards (Hurford, 1990; Galbraith and Laslett, 1993). AFT analysis was carried out at Birkbeck College, University of London, by A.C.

Apatite (U-Th)/He dating methods

For apatite (U-Th)/He analysis, grains free of inclusions and fractures were selected by hand picking using a binocular transmitted light microscope at 60x magnification at Birkbeck College, University of London by C.M. Dimensions and characteristics of selected grains were obtained using a Zeiss Axioplan microscope; grains were then loaded into Pt tubules and degassed by laser heating. He and

U-Th concentrations were measured by quadrupole mass spectrometer. Total uncertainty on sample age is based on reproducibility of the Limberg apatite standard with a reference age of 16.7 ± 1.0 Ma (Kraml et al., 2006) combined with the U-Th and He analytical uncertainties. Age estimates were corrected for α -ejection assuming hexagonal crystal geometry (Ketcham et al., 2011). The standard deviation of the age replicates is used as the error. Ages and isotope concentrations are shown in Table DR4. He degassing and U-Th measurements were carried out at UMR IDES – Université Paris-Sud 11 by C.G.

$^{40}\text{Ar}/^{39}\text{Ar}$ dating methods

For $^{40}\text{Ar}/^{39}\text{Ar}$ dating (Kelley, 2002), unaltered groundmass grains free of phenocrysts or unaltered hornblende grains were selected by hand-picking using a binocular incident light microscope at 20x magnification at the Argon Isotope Facility, SUERC. Samples were loaded in Cu foil and irradiated in the Cd-lined facility of the OSU TRIGA reactor. The samples were irradiated in two separate batches. Samples 27, 31, 40, 41, 44, 47, 48, 52, and F09 were irradiated for 0.383 hours; samples 29 and 34 were irradiated for 0.275 hours. The neutron fluence monitor was Alder Creek Tuff sanidine, with a reference age of 1.193 ± 0.001 Ma (Nomade et al., 2005). Grains were analysed by single crystal total fusion with a focused CO₂ laser. Groundmass samples were step-heated using a resistively heated double-vacuum furnace over a temperature range from 500 to 1750 °C. Isotope data were collected using a GVI ARGUS multi-collector mass spectrometer which has a measured sensitivity of 7×10^{-14} moles volt⁻¹ (Mark et al., 2009). Samples were heated for 5 minutes prior to 10 minutes cleanup. Extracted gases were cleaned using 3 GP50 SAES getters (two operated at 450 °C and one at room temperature) and a cold finger maintained at -95 °C using an acetone-CO_{2(s)} slush trap. The extraction, clean up and data collection processes were entirely automated. Experiments were conducted over 7 hour periods with hot furnace blanks (500 to 1750 °C) collected prior to every sample run. Average backgrounds ± standard deviations were used to correct isotope abundances. Air calibrations were collected in batches ($n = 10$) immediately before and after the individual experiments to monitor mass discrimination. Average $^{40}\text{Ar}/^{36}\text{Ar}$ ratios ± standard deviation (300.08 ± 0.19 , $n = 203$) was used to calculate discrimination factor using the power law. The atmospheric argon ratios of Nier (1950) were

used for discrimination factor determinations, and the decay constants of Steiger and Jager (1977) were utilized. The Berkeley Geochronology Centre software ‘MassSpec’ was used to regress and reduce age data; isotope data are corrected for blank, radioactive decay, mass discrimination and interfering reactions. Plateau calculations are based on the acceptance criteria outlined in Mark et al. (2011): $n = 3$ for minimum number of contiguous steps with no resolvable slope, $F = 0.6$ (that is $> 60\%$ of ^{39}Ar released) and $P = 0.05$ for the probability of fit. Age determinations and isotope measurements and ratios are shown in Table DR5, and step-heating and inverse isochron plots in Figures DR7 and DR8. $^{40}\text{Ar}/^{39}\text{Ar}$ analysis was carried out by C.M. under the supervision of D.M.

Thermal history modelling

We used the HeFTy program (Ketcham, 2005) to model inverse and forward time-temperature (t - T) pathways for piedmont basement samples using standard annealing and diffusion kinetics (see Figure DR2). We reject the use of a model incorporating the effects of radiation damage due to the young ages of the samples (Gautheron et al., 2009). For each sample, random t - T paths are generated; those which acceptably reproduce AFT and AHe ages, and fission track lengths are used to constrain plausible thermal histories. Models include known constraints: AFT ages indicate samples AP1 and AP2 have remained at temperatures below ~ 120 °C since the late Cretaceous; the ~ 20 to ~ 25 Ma onset of Comondú deposition (Umhoefer et al., 2001) indicates samples were within ~ 500 m of the surface at this time; and the presence of a lava yielding an $^{40}\text{Ar}/^{39}\text{Ar}$ ago of ~ 5.7 Ma overlaying the piedmont indicates samples have been at or near the surface since this time.

Infilling canyon lava samples

The Comondú canyon has been completely dammed ~ 15 km west of the escarpment crest by a ~ 6 km long lava flow yielding an $^{40}\text{Ar}/^{39}\text{Ar}$ age of 3.180 ± 0.011 Ma (Figs. 2, 3A-C). Approximately 3 km downstream of the dam, the base of a lava yielding an $^{40}\text{Ar}/^{39}\text{Ar}$ age of 2.585 ± 0.040 Ma is situated ~ 7 m above the modern canyon floor, and a lava flow situated in the modern stream channel immediately downstream of the dam yields an $^{40}\text{Ar}/^{39}\text{Ar}$ age of 0.045 ± 0.009 Ma. Field observations indicate ~ 580 m of vertical incision occurred beneath the relict landscape near the escarpment crest

prior to formation of the ~3.2 Ma lava dam (Fig. 3A-C). Downstream projection of the canyon profile preserved upstream of the dam indicates that only a further ~100 m of vertical incision occurred between ~3.2–2.6 Ma; the canyon has subsequently experienced negligible incision (Fig. 3A-C). Similar age relations are observed in two other canyons. In the San Venancio, a lava flow ~30 km west of the escarpment crest yields an $^{40}\text{Ar}/^{39}\text{Ar}$ age of 2.845 ± 0.009 Ma (Fig. 3A-C). The base of the flow lies ~100 m below the ~14.6–5.6 Ma relict landscape and ~40 m above the modern stream, constraining ~70% of the incision here to before ~2.8 Ma ago. Approximately 14 km downstream, a second lava yields an $^{40}\text{Ar}/^{39}\text{Ar}$ age of 0.426 ± 0.007 Ma; the base lies ~60 m below the relict surface, and ~5 m above the modern stream (Fig. 3A-C). Within the San Javier canyon, a lava ~40 km west of the escarpment yields an $^{40}\text{Ar}/^{39}\text{Ar}$ age of 2.738 ± 0.002 Ma. The base is ~20 m below the relict surface and ~50 m above the modern stream (Fig. 3A-C); the shallow incision depth prior to ~2.7 Ma suggests little uplift occurred this far from the zone of maximum uplift at the Loreto segment faults.

Flexure modelling

A combined topographic/bathymetric profile was obtained from Global Multi-Resolution Topography (GMRT; Ryan et al., 2009) data (horizontal resolution ~100 m), and used to compute the combined mechanical and erosional unloading between the escarpment crest and approximate continent-ocean transition (Lizarralde et al., 2007). Unloading was approximated by a series of columns, with widths of 0.5 km. Deflection produced by each column load i was calculated using the technique of Jordan (1981):

$$w_i = \frac{h}{2} \frac{\rho_c - \rho_w}{\rho_m - \rho_w} \left\{ \exp(-\lambda(-x + s - a)) \cos(\lambda(-x + s - a)) \right. \\ \left. - \exp(-\lambda(-x + s + a)) \cos(\lambda(-x + s + a)) \right\} \quad [S1]$$

where h is load height, ρ_c is continental crust density (2700 kg m^{-3}), ρ_w is seawater density (1025 kg m^{-3}), ρ_m is mantle density (3300 kg m^{-3}), x is horizontal distance, s is the position of the centre of the load, a is the load half-width, and λ is the inverse flexural parameter I/α , where

$$\alpha = \left(\frac{4D}{(\rho_c - \rho_w)g} \right)^{0.25}$$

[S2]

here, g is gravitational acceleration (9.81 m s^{-2}), and D is the flexural rigidity parameter, where

$$D = \frac{ETe^3}{12(1 - \nu^2)}$$

[S3]

here, E is Young's modulus (70 GPa), Te is effective elastic thickness, and ν is Poisson's ratio (0.25).

Total deflection is the sum of deflections from all column loads. The above calculation assumes total replacement of crust by seawater; for replacement by air, ρ_a (1.23 kg m^{-3}) was substituted for ρ_w throughout. The effect of post-rift sediment loading was ignored, as the southern gulf contains little sediment (Lizarralde et al., 2007). Effective elastic thicknesses of 10-15 km give the best matches to observed uplift magnitude, obtained from canyon incision depths (interfluve elevation minus stream elevation), and wavelength see Fig. DR9); this is in agreement with published Te estimates from the northern Gulf (Mueller et al., 2009).

Sample locations

All sample locations are given using WGS84.

REFERENCES CITED IN DATA REPOSITORY:

- Galbraith, R.F., and Laslett, G.M., 1993, Statistical models for mixed fission track ages: Nuclear Tracks and Radiation Measurements, v. 21, no. 4, p. 459–470.
- Gautheron, C., Tassan-Got, L., Barbarand, J., and Pagel, M., 2009, Effect of alpha-damage annealing on apatite (U–Th)/He thermochronology: Chemical Geology, v. 266, no. 3-4, p. 157–170.
- Hurford, A., 1990, Standardization of fission track dating calibration: Recommendation by the Fission Track Working Group of the I.U.G.S. Subcommission on Geochronology: Chemical Geology: Isotope Geoscience section, v. 80, no. 2, p. 171–178, doi: 10.1016/0168-9622(90)90025-8.
- Jordan, T.E., 1981, Thrust loads and foreland basin evolution, Cretaceous, western United States: AAPG Bulletin, v. 65, no. 12, p. 2506–2520.
- Kelley, S., 2002, K-Ar and Ar-Ar Dating, *in* Porcelli, D.P., Ballentine, C.J., and Wieler, R. eds., Noble gases in geochemistry and cosmochemistry, Mineralogical Society of America, p. 785–818.
- Ketcham, R.A., 2005, Forward and Inverse Modeling of Low-Temperature Thermochronometry Data, *in* Reiners, P.W. and Ehlers, T.A. eds., Low-temperature thermochronology: techniques, interpretations, and applications, Mineralogical Society of America, p. 275–314.
- Ketcham, R.A., Gautheron, C., and Tassan-Got, L., 2011, Accounting for long alpha-particle stopping distances in (U–Th–Sm)/He geochronology: Refinement of the baseline case: *Geochimica et Cosmochimica Acta*, v. 75, no. 24, p. 7779–7791, doi: 10.1016/j.gca.2011.10.011.
- Kosler, J., and Sylvester, P.J., 2003, Present Trends and the Future of Zircon in Geochronology: Laser Ablation ICPMS, *in* Hanchar, J.M. and Hoskin, P.W.O. eds., Zircon, Mineralogical Society of America Reviews, p. 243–275.
- Kraml, M., Pik, R., Rahn, M., Selbekk, R., Carignan, J., and Keller, J., 2006, A New Multi-Mineral Age Reference Material for $^{40}\text{Ar}/^{39}\text{Ar}$, (U-Th)/ He and Fission Track Dating Methods: The Limberg t3 Tuff: Geostandards and Geoanalytical Research, v. 30, p. 73–86.
- Lizarralde, D., Axen, G.J., Brown, H.E., Fletcher, J.M., Gonzalez-Fernandez, A., Harding, A.J., Holbrook, W.S., Kent, G.M., Paramo, P., Sutherland, F., and Umhoefer, P.J., 2007, Variation in styles of rifting in the Gulf of California: *Nature*, v. 448, p. 466–469.
- Ludwig, K.R., 2008, Isoplot 3.6: A geochronological toolkit for Microsoft Excel: Berkeley Geochronological Centre Special Publication No.4.,
- Mark, D.F., Barfod, D., Stuart, F.M., and Imlach, J., 2009, The ARGUS multicollector noble gas mass spectrometer: Performance for $^{40}\text{Ar}/^{39}\text{Ar}$ geochronology: *Geochemistry Geophysics Geosystems*, v. 10, doi: 10.1029/2009GC002643.
- Mark, D.F., Rice, C.M., Fallick, A.E., Trewin, N.H., Lee, M.R., Boyce, A., and Lee, J.K.W., 2011, $^{40}\text{Ar}/^{39}\text{Ar}$ dating of hydrothermal activity , biota and gold mineralization in the Rhynie hot-spring system , Aberdeenshire , Scotland: *Geochimica et Cosmochimica Acta*, v. 75, no. 2, p. 555–569, doi: 10.1016/j.gca.2010.10.014.

- Mueller, K., Kier, G., Rockwell, T., and Jones, C.H., 2009, Quaternary rift flank uplift of the Peninsular Ranges in Baja and southern California by removal of mantle lithosphere: *Tectonics*, v. 28.
- Nier, A.O., 1950, A redetermination of the relative abundances of the isotopes of carbon, nitrogen, oxygen, argon, and potassium: *Physical Review*, v. 77, no. 6, p. 789–793.
- Nomade, S., Renne, P., Vogel, N., Deino, A., Sharp, W., Becker, T., Jaouni, A., and Mundil, R., 2005, Alder Creek sanidine (ACs-2): A Quaternary Ar/Ar dating standard tied to the Cobb Mountain geomagnetic event: *Chemical Geology*, v. 218, no. 3-4, p. 315–338, doi: 10.1016/j.chemgeo.2005.01.005.
- Pearce, N.J.G., Perkins, W.T., Westgate, J. A., Gorton, M.P., Jackson, S.E., Neal, C.R., and Chenery, S.P., 1997, A Compilation of New and Published Major and Trace Element Data for NIST SRM 610 and NIST SRM 612 Glass Reference Materials: *Geostandards and Geoanalytical Research*, v. 21, no. 1, p. 115–144, doi: 10.1111/j.1751-908X.1997.tb00538.x.
- Ryan, W.B.F., Carbotte, S.M., Coplan, J.O., O’Hara, S., Melkonian, A., Arko, R., Weissel, R.A., Ferrini, V., Goodwillie, A., Nitsche, F., Bonczkowski, J., and Zemsky, R., 2009, Global Multi-Resolution Topography synthesis: *Geochemistry Geophysics Geosystems*, v. 10, no. 3, doi: 10.1029/2008GC002332.
- Slama, J., Kosler, J., Condon, D., Crowley, J., Gerdes, A., Hanchar, J., Horstwood, M., Morris, G., Nasdala, L., and Norberg, N., 2008, Plešovice zircon — A new natural reference material for U-Pb and Hf isotopic microanalysis: *Chemical Geology*, v. 249, no. 1-2, p. 1–35, doi: 10.1016/j.chemgeo.2007.11.005.
- Steiger, R., and Jager, E., 1977, Subcommission on geochronology: convention on the use of decay constants in geo- and cosmochronology: *Earth and Planetary Science Letters*, v. 36, p. 359–362.
- Umhoefer, P.J., Dorsey, R.J., Willsey, S., Mayer, L., and Renne, P., 2001, Stratigraphy and geochronology of the Comondú Group near Loreto, Baja California Sur, Mexico: *Sedimentary Geology*, v. 144, p. 125–147.

Table DR1: Zircon U-Pb data for basement granodiorite sample AP2, Arroyo Perini, northern transect. Location 26.19102, -111.55077; elevation 136 m asl. Ages shown here were calculated using Glitter v4.4 (www.gitter-gemoc.com) and then further refined using the Microsoft Excel Isoplot plug-in (Ludwig, 2008).

Grain or Standard No.	Isotope Ratios						Ages (Ma)					
	207 Pb/206 Pb	±1σ	206Pb/238 U	±1σ	207 Pb/235 U	±1σ	207 Pb/206 Pb	±1σ	206Pb/238 U	±1σ	207 Pb/235 U	±1σ
GLASS	0.90514	0.01336	0.46717	0.0089	20.96774	9.02763	-	-	-	-	-	-
GLASS2	0.90725	0.00918	0.45149	0.00675	-22.56971	5.67349	-	-	-	-	-	-
STDCZ1	0.05318	0.00052	0.05363	0.00068	0.39124	0.00698	336.6	21.89	336.7	4.15	335.3	5.09
STDCZ2	0.0537	0.00057	0.05473	0.0007	0.40471	0.00767	358.4	23.64	343.5	4.25	345.1	5.55
STDCZ3	0.05293	0.0005	0.05331	0.00067	0.39221	0.00682	325.5	21.4	334.8	4.12	336	4.97
G1	0.11954	0.00699	0.01527	0.00042	0.26367	0.03664	1949.4	100.93	97.7	2.65	237.6	29.44
G2	0.04743	0.00074	0.01393	0.00018	0.08805	0.00167	70.2	37.46	89.2	1.16	85.7	1.56
G3	0.04635	0.00087	0.01423	0.00019	0.09243	0.00222	15.7	43.86	91.1	1.21	89.8	2.07
G4	0.05	0.00179	0.01447	0.00023	0.12385	0.00924	195.2	81.02	92.6	1.48	118.6	8.35
G5	0.04603	0.00218	0.01553	0.00028	0.07963	0.00577	0.1	109.42	99.3	1.76	77.8	5.43
G6	0.0477	0.00149	0.01482	0.00022	0.08117	0.00386	83.8	73.47	94.8	1.43	79.2	3.63
G7	0.05031	0.0014	0.01404	0.00021	0.09004	0.00379	209.4	63.22	89.9	1.32	87.5	3.53
G8	0.05283	0.00113	0.0145	0.0002	0.10402	0.00302	321.3	47.86	92.8	1.27	100.5	2.78
G9	0.05863	0.00306	0.01639	0.00032	0.19325	0.04327	553.4	109.99	104.8	2.05	179.4	36.82
G10	0.04852	0.0024	0.01508	0.00028	0.14337	0.01908	124.8	112.42	96.5	1.76	136	16.95
G11	0.04659	0.00161	0.01391	0.00022	0.07993	0.00361	28.3	81.07	89.1	1.37	78.1	3.39
G12	0.04947	0.00113	0.01347	0.00019	0.09698	0.00296	170.4	52.62	86.2	1.19	94	2.74
G13	0.07115	0.00561	0.01586	0.00046	0.15079	0.02094	961.7	153.25	101.4	2.91	142.6	18.48
G14	0.04819	0.00146	0.01448	0.00022	0.10053	0.00506	108.6	69.97	92.7	1.38	97.3	4.67
G15	-0.00804	0.00241	0.01225	0.00021	-0.01441	0.00437	0.1	0	78.5	1.34	-14.7	4.5

G16	0.05246	0.00169	0.01419	0.00022	0.08956	0.00485	305.4	71.5	90.8	1.39	87.1	4.52
G17	0.04876	0.00086	0.01436	0.00019	0.09117	0.00213	136.3	40.72	91.9	1.21	88.6	1.98
G18	0.05135	0.00147	0.01468	0.00022	0.10642	0.00519	256.4	64.49	94	1.38	102.7	4.76
G19	0.04739	0.00209	0.01531	0.00026	0.11709	0.01252	68.4	102.31	97.9	1.67	112.4	11.38
G20	0.04991	0.00351	0.01632	0.00035	0.06221	0.0079	190.6	155.8	104.3	2.23	61.3	7.55
G21	0.06148	0.00174	0.01533	0.00023	0.13877	0.00748	656	59.67	98	1.47	131.9	6.67
G23	0.04447	0.00228	0.01542	0.00028	0.07867	0.00695	0.1	36.29	98.7	1.8	76.9	6.54
G24	0.05112	0.00206	0.01492	0.00025	0.08938	0.00648	246.4	90.4	95.5	1.6	86.9	6.04
G25	0.04973	0.00259	0.01575	0.0003	0.14485	0.02391	182.6	117.03	100.7	1.89	137.4	21.21
G26	0.05146	0.00299	0.01556	0.00031	0.08904	0.01187	261.3	128.4	99.5	1.97	86.6	11.07
G27	0.05303	0.00275	0.0157	0.00029	0.08349	0.00867	330.2	113.13	100.4	1.87	81.4	8.12
G28	0.05099	0.00263	0.01568	0.0003	0.06176	0.005	240.5	114.8	100.3	1.89	60.9	4.78
G29	0.05038	0.00281	0.0157	0.00031	0.06694	0.00623	212.4	124.27	100.4	1.96	65.8	5.93
G30	0.05047	0.00331	0.01642	0.00035	-0.59921	0.54956	216.7	144.99	105	2.21	-928.4	1392.3
G31	0.07093	0.00387	0.01621	0.00035	0.07701	0.0081	955.3	107.79	103.7	2.2	75.3	7.64
G32	0.05078	0.00336	0.01654	0.00036	0.07098	0.00882	231	145.68	105.7	2.28	69.6	8.36
STDCZ4	0.05296	0.00063	0.05379	0.00068	0.39652	0.00883	327.1	26.71	337.8	4.15	339.1	6.42
STDCZ5	0.05345	0.00063	0.05371	0.00068	0.39211	0.00864	347.7	26.47	337.3	4.14	335.9	6.3
GLASS3	0.90449	0.01135	0.43477	0.00654	123.12579	182.66916	-	-	-	-	-	-

Table DR2: Zircon U-Pb data for basement granodiorite sample SA5, Arroyo San Antonio, southern transect. Location 26.10891, -111.47151; elevation 135 m asl. Ages shown here were calculated using Glitter v4.4 (www.glimmer-gemoc.com) and then further refined using the Microsoft Excel Isoplot plug-in (Ludwig, 2008).

Grain or Standard No.	Isotope Ratios						Ages (Ma)					
	207 Pb/206 Pb	±1σ	206Pb/238 U	±1σ	207 Pb/235 U	±1σ	207 Pb/206 Pb	±1σ	206Pb/238 U	±1σ	207 Pb/235 U	±1σ
STDCZ1	0.05398	0.00056	0.05165	0.00065	0.38113	0.00583	369.9	23.51	324.6	3.96	327.9	4.28
STDCZ2	0.05319	0.00049	0.05371	0.00067	0.38246	0.00538	336.9	20.77	337.3	4.07	328.8	3.95
STDCZ3	0.0529	0.00047	0.05411	0.00067	0.38875	0.0053	324.6	20.03	339.7	4.09	333.5	3.88
G1	0.04838	0.00171	0.01475	0.00023	0.13604	0.00963	118.1	81.3	94.4	1.46	129.5	8.6
G2	0.05104	0.00119	0.01538	0.00021	0.12104	0.00451	242.5	52.99	98.4	1.36	116	4.09
G3	0.02896	0.00229	0.01437	0.00026	0.05515	0.00507	0.1	0	92	1.62	54.5	4.88
G4	0.06704	0.00307	0.016	0.00031	0.43336	0.13071	839.1	92.63	102.3	1.95	365.6	92.59
G5	0.04548	0.00186	0.01543	0.00025	0.15786	0.0178	0.1	65.62	98.7	1.58	148.8	15.61
G6	0.0467	0.00192	0.01572	0.00026	0.09983	0.00785	33.8	95.9	100.6	1.62	96.6	7.25
G7	0.0613	0.00453	0.0172	0.00043	0.11022	0.01833	649.8	151.28	109.9	2.73	106.2	16.76
G8	0.11833	0.00466	0.0167	0.00035	0.33967	0.04849	1931.1	68.91	106.8	2.2	296.9	36.75
G9	0.03643	0.00637	0.01657	0.00056	0.12917	0.04289	0.1	0	106	3.57	123.4	38.56
G10	0.05205	0.00372	0.0161	0.00037	0.83965	0.83476	287.5	155.46	102.9	2.37	619	460.74
G11	0.05006	0.00385	0.01729	0.00042	0.09657	0.01385	197.9	169.33	110.5	2.65	93.6	12.83
G12	0.05838	0.00213	0.01527	0.00025	0.12642	0.00884	544.2	77.97	97.7	1.6	120.9	7.97
G13	0.05686	0.00168	0.01482	0.00023	0.13671	0.0064	485.3	64.54	94.8	1.43	130.1	5.72
G14	0.05013	0.00367	0.01557	0.00037	0.0943	0.01216	201.2	161.66	99.6	2.38	91.5	11.28
G15	0.04828	0.00319	0.01561	0.00034	0.12428	0.01719	112.9	148.75	99.9	2.18	118.9	15.52
G16	0.06003	0.00216	0.0154	0.00026	0.11935	0.00809	604.6	76.12	98.5	1.62	114.5	7.34
G17	0.049	0.00142	0.01499	0.00022	0.12519	0.00668	148	66.42	95.9	1.4	119.8	6.03

G18	0.04785	0.002	0.01561	0.00026	0.12213	0.01129	90.9	96.96	99.9	1.65	117	10.21
G19	0.05706	0.00209	0.01529	0.00025	0.10196	0.00675	493.3	79.29	97.8	1.59	98.6	6.22
G20	0.05529	0.00362	0.01736	0.00037	0.05894	0.0063	424	139.8	111	2.34	58.1	6.04
G21	0.05749	0.00223	0.01587	0.00027	0.1456	0.01445	509.9	83.65	101.5	1.7	138	12.81
G22	0.05846	0.00382	0.01725	0.00039	0.29346	0.09973	547.2	136.56	110.2	2.48	261.3	78.29
G23	0.06359	0.00315	0.01614	0.00031	0.12175	0.01348	728	101.73	103.2	2	116.7	12.2
G24	0.05667	0.0024	0.01556	0.00027	0.10182	0.00785	477.8	91.62	99.6	1.74	98.5	7.24
G25	0.16557	0.00697	0.01815	0.00043	0.31342	0.05299	2513.4	69.13	116	2.72	276.8	40.97
G26	0.05455	0.00311	0.01656	0.00034	0.20704	0.04913	393.6	122.63	105.9	2.13	191.1	41.32
G27	0.06805	0.00296	0.01575	0.00029	0.17287	0.02143	870.2	87.68	100.7	1.85	161.9	18.56
G28	0.07422	0.00309	0.01656	0.00031	0.14389	0.01472	1047.4	81.72	105.9	1.94	136.5	13.06
G29	0.19301	0.00733	0.01526	0.00033	0.46805	0.03667	2768	61	97.7	2.09	389.8	25.36
G30	0.06032	0.00358	0.01679	0.00037	0.34592	0.11976	614.9	123.18	107.4	2.32	301.6	90.35
STDCZ4	0.05122	0.00078	0.05436	0.0007	0.4319	0.01098	250.8	34.85	341.2	4.31	364.5	7.78
G31	0.06473	0.0027	0.0155	0.00028	0.13399	0.01266	765.6	85.52	99.1	1.76	127.7	11.34
G32	0.06219	0.0026	0.01587	0.00029	0.25863	0.03704	680.8	86.85	101.5	1.82	233.6	29.88
STDCZ5	0.05362	0.00049	0.05475	0.00068	0.4454	0.00742	355.1	20.65	343.6	4.15	374	5.21
GLASS2	0.89433	0.00856	0.43682	0.00631	19.03004	3.44187	-	-	-	-	-	-

Table DR3: Apatite fission track data for samples from Arroyo San Antonio (southern transect) and Arroyo Perini (northern transect). Note that sample AP3 was not analysed. Track length data for Arroyo San Antonio samples (SA- sample series, southern transect) could not be obtained. Track densities are ($\times 10^6$ tr cm $^{-2}$) based on number of tracks counted (Nd, Ns, Ni); analyses were by external detector method using 0.5 for the $4\pi/2\pi$ geometry correction factor; ages calculated using dosimeter glass CN-5, (apatite) $\zeta_{CN5} = 339 \pm 5$, calibrated by multiple analyses of IUGS apatite and zircon age standards (Hurford, 1990); $P\chi^2$ is probability for obtaining χ^2 value for v degrees of freedom, where v = no. crystals – 1; central age is a modal age, weighted for different precisions of individual crystals (Galbraith and Laslett, 1993). Sample locations and elevations are as given in Table DR4.

Sample	No. of grains	Dosimeter		Spontaneous		Induced		$P\chi^2$	RE %	Central age (Ma $\pm 1\sigma$)	Mean track length (μm)	$\pm 1\sigma$	No. of tracks	D_{par} (μm)
		ρd	Nd	ρs	Ns	ρi	Ni							
SA2	25	1.422	5911	0.135	148	1.427	1449	8.1	25.8	25.1 \pm 2.6	-	-	-	-
SA3	30	1.422	5911	0.129	105	1.859	1486	64.2	10.5	17.0 \pm 1.8	-	-	-	-
SA4	20	1.422	5911	0.066	69	0.685	752	47.4	8.8	22.1 \pm 2.8	-	-	-	-
SA5	30	1.422	5911	0.073	108	0.790	1223	99.2	0.0	21.2 \pm 2.1	-	-	-	-
AP1	20	1.422	5911	1.663	1250	4.729	3554	67.6	0.3	84.0 \pm 3.0	13.74 \pm 0.11	1.14	100	2.51
AP2	20	1.422	5911	2.283	1656	6.838	4991	73.7	0.1	79.2 \pm 2.5	13.80 \pm 0.11	1.16	110	2.97

Table DR4: Apatite (U-Th)/He data for samples from both Arroyo Perini (AP- sample series, northern transect) and Arroyo San Antonio (SA- sample series, southern transect) samples. F_T is the α particle fraction which is not ejected from the grain (Ketcham et al., 2011). Mean packet age errors are 1σ . The two packet ages marked * are considered anomalous outliers and excluded from analysis.

Sample	Latitude	Longitude	Elevation (m asl)	Packet	No. of xtals	Mass (μg)	U (ppm)	Th (ppm)	He (ncc/mg)	F_T	F_T corrected age (Ma)	Mean packet age $\pm 1\sigma$ (Ma)
AP1	26.18853	-111.56005	140	1	4	3.9	91.5	110.5	58.9	0.63	6.6	6.5 ± 0.4
				2	4	7.7	46.4	55.9	30.4	0.70	6.0	
				3	4	5.1	68.3	77.2	48.5	0.67	6.9	
AP2	26.19102	-111.55077	120	1	3	6.1	105.6	103.6	92.3	0.71	8.3	7.6 ± 0.6
				2	3	4.2	121.7	118.4	84.8	0.67	7.0	
				3	3	3.7	92.2	99.6	68.2	0.66	7.3	
AP3	26.19844	-111.54419	120	1	4	4.6	25.5	39.9	22.2	0.69	7.6	6.9 ± 0.7
				2	3	4.6	48.1	92.6	59.7	0.70	10.0*	
				3	2	3.8	11.5	23.7	10.2	0.71	6.9	
				4	2	7.5	21.5	31.2	17.0	0.80	6.1	
SA2	26.09375	-111.49075	200	1	3	3.8	27.9	39.0	16.4	0.66	5.5	4.8 ± 0.7
				2	3	4.3	29.7	35.8	13.0	0.66	4.1	
				3	2	3.2	18.0	38.5	9.5	0.68	4.2	
				4	2	5.0	27.9	33.9	17.0	0.73	5.3	
SA3	26.09373	-111.48278	170	1	3	2.4	34.1	48.4	12.7	0.61	3.8	5.0 ± 0.8
				2	3	3.4	17.0	23.2	9.3	0.68	5.0	
				3	3	7.2	16.4	24.5	10.5	0.71	5.5	
				4	3	4.2	21.3	34.0	12.9	0.66	5.5	
SA4	26.10193	-111.47810	160	1	4	4.9	18.0	31.3	11.0	0.68	5.3	5.1 ± 0.3
				2	2	6.5	12.4	24.6	8.0	0.75	4.9	
				3	4	1.9	57.5	109.1	57.3	0.54	10.6*	
SA5	26.10891	-111.47151	160	1	3	7.1	13.5	18.9	6.7	0.74	4.2	4.8 ± 0.6
				2	2	10.8	16.9	26.2	11.8	0.77	5.5	
				3	3	8.3	15.8	23.8	9.5	0.79	4.6	

Table DR5: $^{40}\text{Ar}/^{39}\text{Ar}$ data. Samples were irradiated in the Cd-lined facility of the OSU TRIGA reactor. Neutron fluence monitor was Alder Creek Tuff sanidine, with a reference age of 1.193 ± 0.001 Ma (Nomade et al., 2005). Data were also collected using an ARGUS multi-collector noble gas mass spectrometer (Mark et al., 2009). Nucleogenic production ratios: $(^{36}\text{Ar}/^{37}\text{Ar})_{\text{Ca}} = 2.65 \pm 0.2 \times 10^{-4}$; $(^{39}\text{Ar}/^{37}\text{Ar})_{\text{Ca}} = 6.95 \pm 0.9 \times 10^{-4}$; $(^{38}\text{Ar}/^{37}\text{Ar})_{\text{Ca}} = 0.196 \pm 0.08 \times 10^{-4}$; $(^{40}\text{Ar}/^{39}\text{Ar})_{\text{K}} = 7.30 \pm 9.2 \times 10^{-4}$; $(^{36}\text{Ar}/^{38}\text{Ar})_{\text{K}} = 1.22 \times 10^{-2}$; $(^{36}\text{Ar}/^{38}\text{Ar})_{\text{Cl}} = 2.63 \pm 0.02 \times 10^2$; $^{37}\text{Ar}/^{39}\text{Ar}$ to Ca/K = 1.96. Isotopic constants and decay rates: $\lambda(^{40}\text{K}_e)/\text{yr} = 5.81 \pm 0.04 \times 10^{-11}$; $\lambda(^{40}\text{K}_\beta)/\text{yr} = 4.962 \pm 0.00043 \times 10^{-10}$; $\lambda(^{37}\text{Ar})/\text{d} = 1.975 \times 10^{-2}$; $\lambda(^{39}\text{Ar})/\text{d} = 7.068 \times 10^{-6}$; $\lambda(^{36}\text{Cl})/\text{d} = 6.308 \times 10^{-9}$; $(^{40}\text{Ar}/^{36}\text{Ar})_{\text{Atm}} = 295.5 \pm 0.5$; $(^{40}\text{Ar}/^{38}\text{Ar})_{\text{Atm}} = 1575 \pm 2$.

Step ID	Relative Isotopic Abundances								Derived Results								Inverse Isochron Data							
	^{40}Ar $\pm 1\sigma$		^{39}Ar $\pm 1\sigma$		^{38}Ar $\pm 1\sigma$		^{37}Ar $\pm 1\sigma$		^{36}Ar $\pm 1\sigma$		^{39}Ar Mol	^{39}Ar % of total	% (^{36}Ar) _{Ca}	Ca/K $\pm 1\sigma$	% $^{40}\text{Ar}^*$	Age (Ma) $\pm 1\sigma$	w/ $\pm J$	$^{36}\text{Ar}/^{40}\text{Ar}$ $\pm \% 1\sigma$	$^{39}\text{Ar}/^{40}\text{Ar}$ $\pm \% 1\sigma$	$^{36}\text{Ar}/^{39}\text{Ar}$ Er. Corr.				
Sample 27, 6.194 ± 0.014 Ma, 25.83250, -111.46167, EK62, [24], Packet 13, 400 mg groundmass, $J = 0.0163 \times 10^{-3} \pm 3.0 \times 10^{-8}$ (1σ)																								
50630-1	4221.9	2.5	4.691	0.008	2.092	0.006	2.037	0.015	10.928	0.010	3.28E-15	9.1	0.005	0.851	0.006	23.5	6.219	0.045	0.05	0.199	0.00259	0.00111	0.183	0.57
50630-2	2929.4	1.7	4.759	0.005	1.254	0.004	2.156	0.012	6.490	0.005	3.33E-15	9.2	0.009	0.888	0.005	34.5	6.247	0.027	0.03	0.194	0.00222	0.00162	0.129	0.66
50630-3	3745	2.4	9.336	0.005	1.205	0.003	3.560	0.011	6.012	0.006	6.54E-15	18.1	0.016	0.747	0.002	52.6	6.195	0.015	0.02	0.205	0.00161	0.00249	0.089	0.69
50630-4	589.88	0.6	1.099	0.004	0.233	0.003	0.381	0.010	1.209	0.003	7.69E-16	2.1	0.008	0.679	0.018	39.5	6.222	0.041	0.04	0.328	0.00205	0.00186	0.369	0.27
50630-5	3897.2	2.5	12.719	0.006	0.900	0.003	4.130	0.012	4.129	0.004	8.90E-15	24.7	0.026	0.637	0.002	68.7	6.184	0.010	0.02	0.209	0.00106	0.00326	0.087	0.68
50630-6	1936.8	1.2	5.492	0.005	0.547	0.004	1.812	0.012	2.636	0.004	3.84E-15	10.7	0.018	0.647	0.004	59.8	6.196	0.014	0.02	0.225	0.00136	0.00283	0.116	0.60
50630-7	1280.7	0.9	3.125	0.004	0.426	0.003	1.189	0.011	2.107	0.003	2.19E-15	6.1	0.015	0.746	0.007	51.4	6.188	0.019	0.02	0.00164	0.00164	0.00244	0.162	0.52
50630-8	1381.1	1.0	2.736	0.005	0.544	0.004	1.583	0.012	2.806	0.003	1.92E-15	5.3	0.015	1.134	0.009	40.0	5.929	0.025	0.03	0.00203	0.00203	0.00198	0.182	0.54
50630-9	2052.5	1.2	6.394	0.005	0.541	0.003	19.417	0.021	2.587	0.004	4.48E-15	12.4	0.199	5.952	0.008	62.8	5.936	0.012	0.02	0.00126	0.00126	0.00311	0.110	0.58
50630-10	517.33	0.6	1.198	0.004	0.186	0.003	3.897	0.011	0.898	0.003	8.39E-16	2.3	0.115	6.374	0.027	48.8	6.198	0.036	0.04	0.00173	0.00173	0.00231	0.332	0.26

Step ID	Relative Isotopic Abundances									Derived Results							Inverse Isochron Data							
	^{40}Ar		^{39}Ar		^{38}Ar		^{37}Ar		^{36}Ar		^{39}Ar Mol	^{39}Ar % of total	$\%(^{36}\text{Ar})_{\text{Ca}}$	Ca/K $\pm 1\sigma$	$\%^{40}\text{Ar}^*$	Age (Ma) $\pm 1\sigma$	w/ $\pm J$	$^{36}\text{Ar}/^{40}\text{Ar}$ $\pm 1\sigma$	$^{39}\text{Ar}/^{40}\text{Ar}$ $\pm 1\sigma$	$^{36}\text{Ar}/^{39}\text{Ar}$ Er. Corr.				
Sample 31, 2.845 ± 0.009 Ma, 25.88395 -111.77107, EK62, [25], Packet 16, 400 mg groundmass, $J = 0.0122 \times 10^{-3} \pm 2.0 \times 10^{-8}$ (1σ)																								
50633-1	4195.5	2.4	0.969	0.013	2.632	0.009	0.653	0.017	14.037	0.01	6.79E-16	3.4	0.001	1.32	0.04	1.1	1.079	0.184	0.18	0.19	0.00335	1.37	0.000	0.1143
50633-2	3106.6	1.8	1.861	0.007	1.834	0.005	2.058	0.011	9.821	0.00	1.30E-15	6.6	0.006	2.17	0.01	6.6	2.420	0.069	0.07	0.20	0.00316	0.37	0.001	0.3710
50633-3	2047	1.2	2.114	0.005	1.132	0.003	2.256	0.008	6.015	0.00	1.48E-15	7.5	0.010	2.09	0.01	13.2	2.810	0.039	0.04	0.20	0.00294	0.23	0.001	0.5095
50633-4	1715.1	1.0	2.639	0.004	0.891	0.003	2.447	0.008	4.654	0.00	1.85E-15	9.3	0.014	1.82	0.01	19.8	2.835	0.025	0.03	0.21	0.00271	0.18	0.002	0.5591
50633-5	2167.9	1.2	4.741	0.005	1.018	0.004	3.605	0.009	5.262	0.00	3.32E-15	16.7	0.018	1.49	0.00	28.3	2.846	0.016	0.02	0.20	0.00243	0.12	0.002	0.6653
50633-6	1215.5	0.8	2.698	0.004	0.570	0.003	1.777	0.007	2.943	0.00	1.89E-15	9.5	0.016	1.29	0.01	28.5	2.823	0.017	0.02	0.21	0.00242	0.17	0.002	0.5587
50633-7	2134.3	1.3	5.627	0.004	0.936	0.003	4.056	0.009	4.758	0.00	3.94E-15	19.8	0.023	1.41	0.00	34.1	2.849	0.013	0.01	0.20	0.00223	0.10	0.003	0.6765
50633-8	1373.2	0.8	2.676	0.004	0.669	0.003	2.121	0.008	3.464	0.00	1.87E-15	9.4	0.016	1.55	0.01	25.5	2.874	0.019	0.02	0.20	0.00252	0.18	0.002	0.5742
50633-9	2180.3	1.3	3.010	0.005	1.154	0.003	2.490	0.008	6.100	0.00	2.11E-15	10.6	0.011	1.62	0.01	17.3	2.763	0.029	0.03	0.20	0.00280	0.17	0.001	0.5764
50633-10	1672.7	1.0	1.359	0.005	0.956	0.003	1.460	0.008	5.102	0.00	9.51E-16	4.8	0.008	2.11	0.01	9.9	2.675	0.051	0.05	0.20	0.00305	0.35	0.001	0.3835
50633-11	1173.7	0.7	0.475	0.004	0.709	0.002	13.285	0.014	3.799	0.00	3.32E-16	1.7	0.093	54.84	0.50	4.4	2.460	0.110	0.11	0.20	0.00323	0.96	0.000	0.1603
50633-12	707.26	0.5	0.201	0.004	0.434	0.003	9.678	0.011	2.316	0.00	1.41E-16	0.7	0.111	94.25	1.88	3.3	2.658	0.194	0.19	0.24	0.00327	2.11	0.000	0.0642

Step ID	Relative Isotopic Abundances								Derived Results								Inverse Isochron Data							
	^{40}Ar		^{39}Ar		^{38}Ar		^{37}Ar		^{36}Ar		^{39}Ar Mol	^{39}Ar % of total	% $(^{36}\text{Ar})_{\text{Ca}}$	Ca/K	% $^{40}\text{Ar}^*$	Age (Ma)	w/ $\pm J$	$^{36}\text{Ar}/^{40}\text{Ar}$	$^{39}\text{Ar}/^{40}\text{Ar}$	$^{36}\text{Ar}/^{39}\text{Ar}$ Er. Corr.				
$\pm 1\sigma$		$\pm 1\sigma$		$\pm 1\sigma$		$\pm 1\sigma$		$\pm 1\sigma$																
Sample 40, 0.426 ± 0.007 Ma, 25.85136 -111.89128, EK62, Packet 14, 400 mg groundmass, $J = 0.013 \times 10^{-3} \pm 3.0 \times 10^{-8}$ (1σ)																								
50627-1	1765.2	1.6	2.977	0.140	1.265	0.052	0.690	0.121	5.907	0.007	2.08E-15	4.7	0.003	0.454	0.082	1.1	0.158	0.033	0.03	0.23	0.00335	4.65	0.00169	0.03
50627-2	2462.5	1.0	4.678	0.009	1.615	0.006	0.724	0.017	8.096	0.006	3.27E-15	7.3	0.002	0.303	0.007	2.8	0.357	0.023	0.02	0.19	0.00329	0.19	0.00190	0.55
50627-3	2553.1	1.5	5.458	0.005	1.624	0.004	0.826	0.011	8.334	0.006	3.82E-15	8.6	0.003	0.297	0.004	3.5	0.395	0.021	0.02	0.19	0.00326	0.11	0.00214	0.69
50627-4	2648.1	1.5	6.931	0.005	1.675	0.004	1.052	0.012	8.550	0.008	4.85E-15	10.9	0.003	0.298	0.003	4.6	0.418	0.017	0.02	0.20	0.00323	0.10	0.00262	0.69
50627-5	2569.9	1.5	7.339	0.005	1.625	0.003	1.157	0.010	8.253	0.008	5.14E-15	11.5	0.004	0.309	0.003	5.1	0.426	0.016	0.02	0.20	0.00321	0.10	0.00286	0.68
50627-6	2621.5	1.6	7.980	0.005	1.651	0.003	1.312	0.010	8.380	0.008	5.59E-15	12.5	0.004	0.322	0.002	5.5	0.434	0.015	0.02	0.20	0.00320	0.10	0.00304	0.69
50627-7	2611.3	1.6	7.716	0.004	1.642	0.004	1.314	0.010	8.366	0.007	5.40E-15	12.1	0.004	0.334	0.003	5.3	0.430	0.015	0.02	0.20	0.00320	0.09	0.00295	0.71
50627-8	2639.5	1.5	6.843	0.005	1.655	0.004	1.192	0.011	8.508	0.007	4.79E-15	10.7	0.004	0.341	0.003	4.8	0.437	0.018	0.02	0.20	0.00322	0.10	0.00259	0.69
50627-9	4561.9	2.8	6.029	0.006	2.860	0.003	1.077	0.010	15.057	0.012	4.22E-15	9.5	0.002	0.350	0.003	2.5	0.445	0.035	0.03	0.20	0.00330	0.13	0.00132	0.66
50627-10	8902.3	5.6	7.777	0.012	5.565	0.006	1.674	0.011	29.472	0.022	5.44E-15	12.2	0.002	0.422	0.003	2.2	0.592	0.052	0.05	0.19	0.00331	0.17	0.00087	0.61

Step ID	Relative Isotopic Abundances										Derived Results								Inverse Isochron Data					
	^{40}Ar		^{39}Ar		^{38}Ar		^{37}Ar		^{36}Ar		^{39}Ar Mol	^{39}Ar % of total	% (^{36}Ar) _{Ca}	Ca/K $\pm 1\sigma$	% $^{40}\text{Ar}^*$	Age (Ma) $\pm 1\sigma$	w/ $\pm J$	$^{36}\text{Ar}/^{40}\text{Ar}$	$^{39}\text{Ar}/^{40}\text{Ar}$	$^{36}\text{Ar}/^{39}\text{Ar}$ Er. Corr.				
Sample 44, 0.045 ± 0.009 Ma, 26.06966 -111.79287, EK62, [23], Packet 11, 400 mg groundmass, $J = 0.0165 \times 10^{-3} \pm 3.0 \times 10^{-8}$ (1σ)																								
50614-1	528.7	0.5	1.531	0.008	0.368	0.005	0.300	0.010	1.722	0.005	1.07E-15	4.2	0.00	0.384	0.012	3.8	0.389	0.034	0.03	0.003	0.34	0.003	0.52	0.18
50614-2	1307.2	0.7	4.375	0.006	0.886	0.003	1.051	0.007	4.373	0.006	3.06E-15	12.1	0.01	0.471	0.003	1.2	0.102	0.020	0.02	0.003	0.22	0.003	0.14	0.55
50614-3	914.0	0.5	3.046	0.005	0.618	0.004	0.810	0.007	3.066	0.005	2.13E-15	8.4	0.01	0.521	0.004	0.9	0.078	0.021	0.02	0.003	0.24	0.003	0.19	0.46
50614-4	1766.0	1.1	6.719	0.004	1.198	0.003	2.574	0.007	5.957	0.007	4.70E-15	18.5	0.01	0.751	0.002	0.3	0.026	0.016	0.02	0.003	0.21	0.004	0.10	0.66
50614-5	780.2	0.5	2.619	0.004	0.529	0.003	1.143	0.007	2.617	0.006	1.83E-15	7.2	0.01	0.855	0.005	0.9	0.077	0.025	0.03	0.003	0.29	0.003	0.18	0.40
50614-6	473.6	0.3	1.436	0.004	0.321	0.003	0.638	0.006	1.601	0.005	1.01E-15	4.0	0.01	0.871	0.009	0.1	0.012	0.035	0.03	0.003	0.35	0.003	0.29	0.25
50614-7	1747.4	1.1	6.165	0.005	1.175	0.003	3.609	0.008	5.895	0.007	4.32E-15	17.0	0.02	1.147	0.003	0.3	0.027	0.018	0.02	0.003	0.21	0.004	0.11	0.64
50614-8	1253.1	0.8	3.490	0.005	0.833	0.003	2.182	0.007	4.220	0.006	2.44E-15	9.6	0.01	1.225	0.004	0.5	0.054	0.024	0.02	0.003	0.23	0.003	0.16	0.54
50614-9	1712.6	1.0	3.927	0.005	1.127	0.003	2.348	0.006	5.772	0.006	2.75E-15	10.8	0.01	1.172	0.003	0.4	0.054	0.027	0.03	0.003	0.21	0.002	0.13	0.62
50614-10	4173.9	2.6	2.926	0.008	2.652	0.003	1.498	0.008	14.107	0.013	2.05E-15	8.1	0.00	1.004	0.006	0.1	0.055	0.085	0.09	0.003	0.20	0.001	0.27	0.47

Step ID	Relative Isotopic Abundances								Derived Results								Inverse Isochron Data							
	^{40}Ar		^{39}Ar		^{38}Ar		^{37}Ar		^{36}Ar		^{39}Ar Mol	^{39}Ar % of total	% (^{36}Ar) _{ca}	Ca/K $\pm 1\sigma$	% $^{40}\text{Ar}^*$	Age (Ma) $\pm 1\sigma$	w/ $\pm J$	$^{36}\text{Ar}/^{40}\text{Ar}$	$^{39}\text{Ar}/^{40}\text{Ar}$	$^{36}\text{Ar}/^{39}\text{Ar}$ Er. Corr.				
Sample 47, 2.585 ± 0.040 Ma, 26.05968 -111.81866, EK62, [26], Packet 18, 400 mg groundmass, $J = 0.0163 \times 10^{-3} \pm 3.0 \times 10^{-8}$ (1σ)																								
50645-1	4579.2	2.5	1.293	0.043	2.938	0.018	0.513	0.034	15.075	0.014	9.05E-16	13.4	0.00	0.778	0.057	2.7	2.831	0.224	0.22	0.003	0.20	0.0003	3.30	0.05
50645-2	6260.6	3.3	1.897	0.012	3.909	0.005	1.522	0.009	20.622	0.015	1.33E-15	19.6	0.00	1.573	0.013	2.7	2.589	0.182	0.18	0.003	0.19	0.0003	0.60	0.25
50645-3	4802.0	2.8	1.766	0.010	2.968	0.004	2.529	0.009	15.728	0.012	1.24E-15	18.3	0.00	2.807	0.019	3.2	2.576	0.152	0.15	0.003	0.19	0.0004	0.58	0.26
50645-4	3025.6	1.6	1.401	0.009	1.850	0.004	3.263	0.007	9.832	0.008	9.80E-16	14.5	0.01	4.566	0.032	4.0	2.529	0.120	0.12	0.003	0.19	0.0005	0.67	0.22
50645-5	1542.2	0.8	0.939	0.005	0.933	0.003	3.101	0.008	4.938	0.003	6.57E-16	9.7	0.02	6.472	0.040	5.4	2.612	0.089	0.09	0.003	0.19	0.0006	0.57	0.26
50645-6	583.3	0.4	0.414	0.005	0.355	0.002	1.582	0.008	1.854	0.003	2.90E-16	4.3	0.02	7.485	0.092	6.1	2.519	0.095	0.09	0.003	0.23	0.0007	1.12	0.13
50645-7	888.5	0.5	0.955	0.004	0.527	0.003	4.281	0.008	2.723	0.002	6.69E-16	9.9	0.04	8.783	0.042	9.5	2.593	0.052	0.05	0.003	0.20	0.0011	0.45	0.31
50645-8	557.0	0.4	0.478	0.005	0.334	0.002	2.239	0.008	1.759	0.003	3.35E-16	5.0	0.03	9.173	0.092	6.7	2.301	0.085	0.09	0.003	0.25	0.0009	0.96	0.13
50645-9	254.9	0.4	0.189	0.004	0.160	0.002	0.848	0.007	0.819	0.002	1.32E-16	2.0	0.03	8.789	0.198	5.0	2.001	0.132	0.13	0.003	0.33	0.0007	2.10	0.07
50645-10	573.1	0.4	0.323	0.004	0.358	0.002	1.470	0.008	1.883	0.002	2.26E-16	3.3	0.02	8.913	0.108	2.9	1.540	0.114	0.11	0.003	0.22	0.0006	1.10	0.13

Step ID	Relative Isotopic Abundances								Derived Results								Inverse Isochron Data							
	^{40}Ar		^{39}Ar		^{38}Ar		^{37}Ar		^{36}Ar		^{39}Ar Mol	^{39}Ar % of total	% $(^{36}\text{Ar})_{\text{Ca}}$	Ca/K $\pm 1\sigma$	$\%^{40}\text{Ar}^*$	Age (Ma) $\pm 1\sigma$	w/ $\pm J$	$^{36}\text{Ar}/^{40}\text{Ar}$	$^{39}\text{Ar}/^{40}\text{Ar}$	$^{36}\text{Ar}/^{39}\text{Ar}$ Er. Corr.				
$\pm 1\sigma$		$\pm 1\sigma$		$\pm 1\sigma$		$\pm 1\sigma$		$\pm 1\sigma$																
Sample 48, 14.630 ± 0.040 Ma, 26.09669 -111.70546, EK62, [26], Packet 17, 400 mg groundmass, $J = 0.0128 \times 10^{-3} \pm 3.0 \times 10^{-8}$ (1σ)																								
50642-1	3104.3	1.5	1.859	0.010	1.248	0.004	1.419	0.010	6.642	0.006	1.30E-15	5.5	0.006	1.495	0.013	36.8	14.132	0.092	0.10	0.002	0.196	0.001	0.530	0.27
50642-2	2673.9	1.4	2.104	0.008	0.859	0.003	1.412	0.008	4.550	0.005	1.47E-15	6.2	0.008	1.315	0.008	49.7	14.536	0.064	0.07	0.002	0.202	0.001	0.367	0.36
50642-3	2715.7	1.4	2.587	0.006	0.689	0.003	1.505	0.009	3.608	0.003	1.81E-15	7.7	0.011	1.140	0.007	60.7	14.674	0.045	0.05	0.001	0.196	0.001	0.256	0.47
50642-4	4568.1	1.3	5.695	0.024	0.804	0.007	2.708	0.017	3.198	0.003	3.99E-15	16.9	0.022	0.932	0.007	79.3	14.637	0.063	0.07	0.001	0.190	0.001	0.424	0.32
50642-5	3613.3	1.7	4.556	0.012	0.529	0.004	2.103	0.012	2.398	0.002	3.19E-15	13.5	0.023	0.905	0.006	80.4	14.670	0.040	0.05	0.001	0.198	0.001	0.257	0.46
50642-6	4565.8	2.5	5.420	0.014	0.732	0.004	2.361	0.010	3.777	0.003	3.79E-15	16.1	0.017	0.854	0.004	75.6	14.643	0.042	0.05	0.001	0.189	0.001	0.271	0.48
50642-7	3961.7	2.1	3.978	0.014	0.937	0.003	1.645	0.008	4.909	0.004	2.78E-15	11.8	0.009	0.811	0.005	63.4	14.523	0.057	0.06	0.001	0.191	0.001	0.364	0.38
50642-8	5448.8	3.1	6.254	0.012	0.923	0.003	12.118	0.014	4.818	0.004	4.38E-15	18.5	0.067	3.798	0.009	73.9	14.826	0.035	0.05	0.001	0.194	0.001	0.210	0.54
50642-9	1985.4	1.2	1.318	0.007	0.734	0.003	4.079	0.008	3.875	0.004	9.22E-16	3.9	0.028	6.068	0.035	42.3	14.704	0.092	0.10	0.002	0.199	0.001	0.543	0.27

Step ID	Relative Isotopic Abundances								Derived Results								Inverse Isochron Data							
	^{40}Ar		^{39}Ar		^{38}Ar		^{37}Ar		^{36}Ar		^{39}Ar Mol	^{39}Ar % of total	% $(^{36}\text{Ar})_{\text{Ca}}$	Ca/K	% $^{40}\text{Ar}^*$	Age (Ma)	w/ $\pm J$	$^{36}\text{Ar}/^{40}\text{Ar}$	$^{39}\text{Ar}/^{40}\text{Ar}$	$^{36}\text{Ar}/^{39}\text{Ar}$ Er. Corr.				
Sample 52, 5.655 ± 0.152 Ma, 26.17252 -111.56977, EK62, [23], Packet 12, 40 mg hornblende, $J = 0.0101 \times 10^{-3} \pm 2.0 \times 10^{-8}$ (1σ)																								
50616-1	172.1	0.3	0.028	0.004	0.105	0.003	0.045	0.007	0.554	0.003	1.97E-17	5.8	0.002	3.1	0.7	4.9	5.462	1.007	1.01	0.591	0.003	14.451	0.000	0.01
50616-2	83.1	0.3	0.028	0.004	0.043	0.003	0.076	0.005	0.255	0.002	1.95E-17	5.7	0.008	5.3	0.9	9.2	5.010	0.846	0.85	0.843	0.003	14.641	0.000	0.01
50616-3	62.1	0.3	0.045	0.004	0.028	0.002	0.054	0.008	0.164	0.002	3.12E-17	9.2	0.009	2.4	0.4	21.8	5.492	0.551	0.55	1.214	0.003	8.950	0.001	0.02
50616-4	50.3	0.3	0.050	0.003	0.024	0.002	0.060	0.007	0.121	0.001	3.48E-17	10.2	0.013	2.4	0.3	28.9	5.302	0.410	0.41	1.382	0.002	6.823	0.001	0.04
50616-5	146.7	0.3	0.145	0.004	0.066	0.003	0.499	0.020	0.340	0.005	1.01E-16	29.8	0.039	6.7	0.3	31.4	5.781	0.248	0.25	1.530	0.002	2.669	0.001	0.02
50616-6	44.7	0.3	0.063	0.004	0.012	0.002	0.087	0.007	0.081	0.002	4.43E-17	13.0	0.028	2.7	0.3	46.4	5.929	0.410	0.41	2.236	0.002	6.338	0.001	0.04
50616-7	39.7	0.3	0.052	0.004	0.015	0.002	0.040	0.007	0.080	0.002	3.64E-17	10.7	0.013	1.5	0.3	40.2	5.582	0.484	0.48	2.891	0.002	7.440	0.001	0.03
50616-8	59.4	0.3	0.039	0.003	0.027	0.003	0.046	0.006	0.159	0.001	2.71E-17	8.0	0.008	2.3	0.4	21.0	5.845	0.569	0.57	1.080	0.003	8.750	0.001	0.03
50616-9	60.8	0.3	0.037	0.004	0.026	0.003	0.071	0.006	0.167	0.002	2.60E-17	7.7	0.011	3.8	0.5	18.7	5.549	0.703	0.70	1.155	0.003	11.552	0.001	0.02
50616-1	172.1	0.3	0.028	0.004	0.105	0.003	0.045	0.007	0.554	0.003	1.97E-17	5.8	0.002	3.1	0.7	4.9	5.462	1.007	1.01	0.591	0.003	14.451	0.000	0.01

Step ID	Relative Isotopic Abundances								Derived Results								Inverse Isochron Data							
	^{40}Ar		^{39}Ar		^{38}Ar		^{37}Ar		^{36}Ar		^{39}Ar Mol	^{39}Ar % of total	% $(^{36}\text{Ar})_{\text{Ca}}$	Ca/K	$\% \text{ }^{40}\text{Ar}^*$	Age (Ma)	w/ $\pm J$	$^{36}\text{Ar}/^{40}\text{Ar}$	$^{39}\text{Ar}/^{40}\text{Ar}$	$^{36}\text{Ar}/^{39}\text{Ar}$ Er. Corr.				
Sample F09, 3.180 ± 0.011 Ma, 26.07995 -111.76418, EK62, [23], Packet 10, 400 mg groundmass, $J = 0.0151 \times 10^{-3} \pm 3.0 \times 10^{-8}$ (1 σ)																								
50612-1	2881.9	1.7	2.020	0.007	1.684	0.004	0.917	0.010	8.940	0.008	1.41E-15	4.1	0.003	0.889	0.010	8.3	3.239	0.073	0.07	0.199	0.003	0.328	0.001	0.40
50612-2	3147.5	1.8	3.378	0.005	1.763	0.004	1.716	0.009	9.308	0.007	2.36E-15	6.9	0.005	0.996	0.005	12.6	3.203	0.044	0.04	0.191	0.003	0.168	0.001	0.61
50612-3	3004.6	1.7	4.596	0.005	1.596	0.004	2.150	0.012	8.364	0.006	3.22E-15	9.4	0.007	0.917	0.005	17.7	3.160	0.030	0.03	0.191	0.003	0.121	0.002	0.68
50612-4	2754.2	1.6	5.447	0.004	1.376	0.004	2.101	0.010	7.162	0.006	3.81E-15	11.2	0.008	0.756	0.004	23.2	3.191	0.023	0.02	0.198	0.003	0.098	0.002	0.69
50612-5	2905.7	1.7	6.754	0.005	1.396	0.004	2.223	0.009	7.176	0.005	4.73E-15	13.8	0.008	0.645	0.003	27.0	3.168	0.018	0.02	0.189	0.002	0.100	0.002	0.72
50612-6	2722.7	1.6	6.396	0.004	1.307	0.004	1.959	0.010	6.701	0.005	4.48E-15	13.1	0.008	0.600	0.003	27.3	3.163	0.018	0.02	0.193	0.002	0.095	0.002	0.72
50612-7	2491.0	1.4	5.558	0.004	1.217	0.004	1.772	0.010	6.236	0.005	3.89E-15	11.4	0.008	0.625	0.003	26.0	3.178	0.020	0.02	0.197	0.003	0.096	0.002	0.70
50612-8	3786.1	2.3	6.073	0.004	1.986	0.004	2.351	0.011	10.370	0.008	4.25E-15	12.4	0.006	0.759	0.004	19.1	3.239	0.029	0.03	0.196	0.003	0.097	0.002	0.71
50612-9	2788.8	1.6	2.837	0.005	1.562	0.004	1.558	0.010	8.224	0.007	1.99E-15	5.8	0.005	1.077	0.007	12.9	3.447	0.048	0.05	0.197	0.003	0.181	0.001	0.58
50612-10	1716.6	1.0	2.192	0.004	0.940	0.004	10.674	0.013	4.893	0.005	1.53E-15	4.5	0.058	9.543	0.021	15.8	3.384	0.039	0.04	0.205	0.003	0.204	0.001	0.52

Step ID	Relative Isotopic Abundances										Derived Results								Inverse Isochron Data						
	^{40}Ar ± 1σ		^{39}Ar ± 1σ		^{38}Ar ± 1σ		^{37}Ar ± 1σ		^{36}Ar ± 1σ		^{39}Ar Mol	^{39}Ar % of total	% (^{36}Ar) _{Ca}	Ca/K ± 1σ	% $^{40}\text{Ar}^*$	Age (Ma) ± 1σ	w/±J	$^{36}\text{Ar}/^{40}\text{Ar}$ ± %1σ	$^{39}\text{Ar}/^{40}\text{Ar}$ ± %1σ	$^{36}\text{Ar}/^{39}\text{Ar}$ Ar Er. Corr.					
Sample 29, 5.592 ± 0.003 Ma, 25.97035 -111.67056, EK63, Packet 35, 400 mg groundmass, $J = 0.078 \times 10^{-3} \pm 1.0 \times 10^{-8}$ (1σ)																									
61083-1	1515.7	2.3	6.444	0.110	1.133	0.050	0.775	0.043	4.281	0.005	4.51E-15	1.9	0.03	1.231	0.071	16.6	5.480	0.160	0.16	0.443	0.003	1.70	0.00	4	0.23
61083-2	925.4	0.5	16.626	0.021	0.367	0.004	1.487	0.006	0.845	0.003	1.16E-14	4.8	0.24	0.915	0.004	73.1	5.723	0.018	0.02	0.558	0.001	0.17	0.01	2	0.56
61083-3	748.9	0.4	15.804	0.017	0.252	0.003	1.245	0.005	0.361	0.003	1.11E-14	4.6	0.48	0.806	0.003	85.8	5.723	0.015	0.02	0.979	0.000	0.15	0.02	8	0.32
61083-4	2434.7	1.5	57.57	0.050	0.717	0.003	2.527	0.005	0.383	0.003	4.03E-14	16.6	0.92	0.450	0.001	95.4	5.675	0.009	0.01	0.963	0.000	0.14	0.02	6	0.33
61083-5	2991.7	1.7	71.537	0.059	0.87	0.004	2.813	0.005	0.377	0.003	5.01E-14	20.6	1.04	0.403	0.008	96.3	5.666	0.009	0.01	0.999	0.000	0.14	0.02	1	0.32
61083-6	3114.5	1.8	75.005	0.062	0.908	0.003	3.067	0.005	0.314	0.003	5.25E-14	21.6	1.35	0.420	0.001	97.1	5.669	0.009	0.01	1.142	0.000	0.14	0.02	2	0.28
61083-7	2075.7	1.2	49.79	0.041	0.613	0.004	2.174	0.004	0.241	0.003	3.49E-14	14.4	1.25	0.448	0.001	96.6	5.665	0.009	0.01	1.431	0.000	0.14	0.02	2	0.22
61083-8	1470.8	0.8	34.702	0.032	0.451	0.004	1.683	0.004	0.251	0.003	2.43E-14	10.0	0.93	0.498	0.001	95.0	5.664	0.010	0.01	1.375	0.000	0.14	0.02	7	0.23
61083-9	841.2	0.5	19.221	0.016	0.279	0.003	1.126	0.004	0.244	0.004	1.35E-14	5.5	0.64	0.601	0.002	91.5	5.632	0.012	0.01	1.520	0.000	0.14	0.02	3	0.21

Step ID	Relative Isotopic Abundances								Derived Results								Inverse Isochron Data			
	^{40}Ar		^{39}Ar		^{38}Ar		^{37}Ar		^{36}Ar		^{39}Ar Mol	^{39}Ar % of total	% (^{36}Ar) Ca	Ca/K $\pm 1\sigma$	% ^{40}Ar *	Age (Ma) $\pm 1\sigma$	w/ $\pm J$	$^{36}\text{Ar}/^{40}\text{Ar}$ $\pm \% 1\sigma$	$^{39}\text{Ar}/^{40}\text{Ar}$ $\pm \% 1\sigma$	$^{36}\text{Ar}/^{39}\text{Ar}$ Er. Corr.
Sample 34, 2.738 ± 0.002 Ma, 25.55603 -111.72045, EK63, Packet 34, 400 mg groundmass, $J = 0.079 \times 10^{-3} \pm 8.0 \times 10^{-8}$ (1σ)																				
61085-1	3459.6	28.000	13.57	0.76	3.053	0.260	1.096	0.210	10.9	0.053	9.50E-15	3.6	0.01	0.811	0.16	6.2	2.24	0.3	0.38	1.01
61085-2	2335.0	1.402	78.93	0.08	1.429	0.004	1.232	0.004	2.64	7	0.004	5.53E-14	21.1	0.06	0.157	0.00	2.80	0.0	0.42	0.15
61085-3	2145.9	1.202	83.01	0.08	1.290	0.004	0.888	0.004	1.71	4	0.003	5.81E-14	22.2	0.07	0.108	0.00	2.81	0.0	0.44	0.14
61085-4	1590.4	1.003	62.25	0.06	0.956	0.004	0.628	0.003	1.21	8	0.003	4.36E-14	16.6	0.07	0.101	0.00	2.81	0.0	0.48	0.15
61085-5	1007.4	0.495	38.08	0.04	0.610	0.003	0.417	0.003	0.86	0	0.003	2.67E-14	10.2	0.07	0.110	0.00	2.82	0.0	0.56	0.14
61085-6	811.8	0.396	31.18	0.03	0.486	0.003	0.379	0.003	0.65	4	0.003	2.18E-14	8.3	0.08	0.122	0.00	2.82	0.0	0.63	0.14
61085-7	685.2	0.357	26.39	0.03	0.408	0.004	0.389	0.003	0.55	3	0.003	1.85E-14	7.0	0.10	0.149	0.00	2.82	0.0	0.67	0.15
61085-8	580.5	0.357	22.88	0.02	0.354	0.003	0.405	0.004	0.43	5	0.003	1.60E-14	6.1	0.13	0.178	0.00	2.81	0.0	0.80	0.15
61085-9	635.5	0.338	15.76	0.02	0.410	0.003	11.233	0.011	1.12	4	0.003	1.10E-14	4.2	1.37	7.195	0.01	2.79	0.0	0.50	0.15
61085-10	135.5	0.080	2.40	0.01	0.089	0.003	3.210	0.004	0.30	8	0.003	1.68E-15	0.6	1.42	13.504	0.04	2.72	0.0	1.04	0.29
															1	33.7	6	57	0.06	2
																		0.002	7	18
																			0.3	

Figure DR1: Zircon U-Pb concordia. Age estimates were calculated using Isoplot v3.6 (Ludwig, 2008).

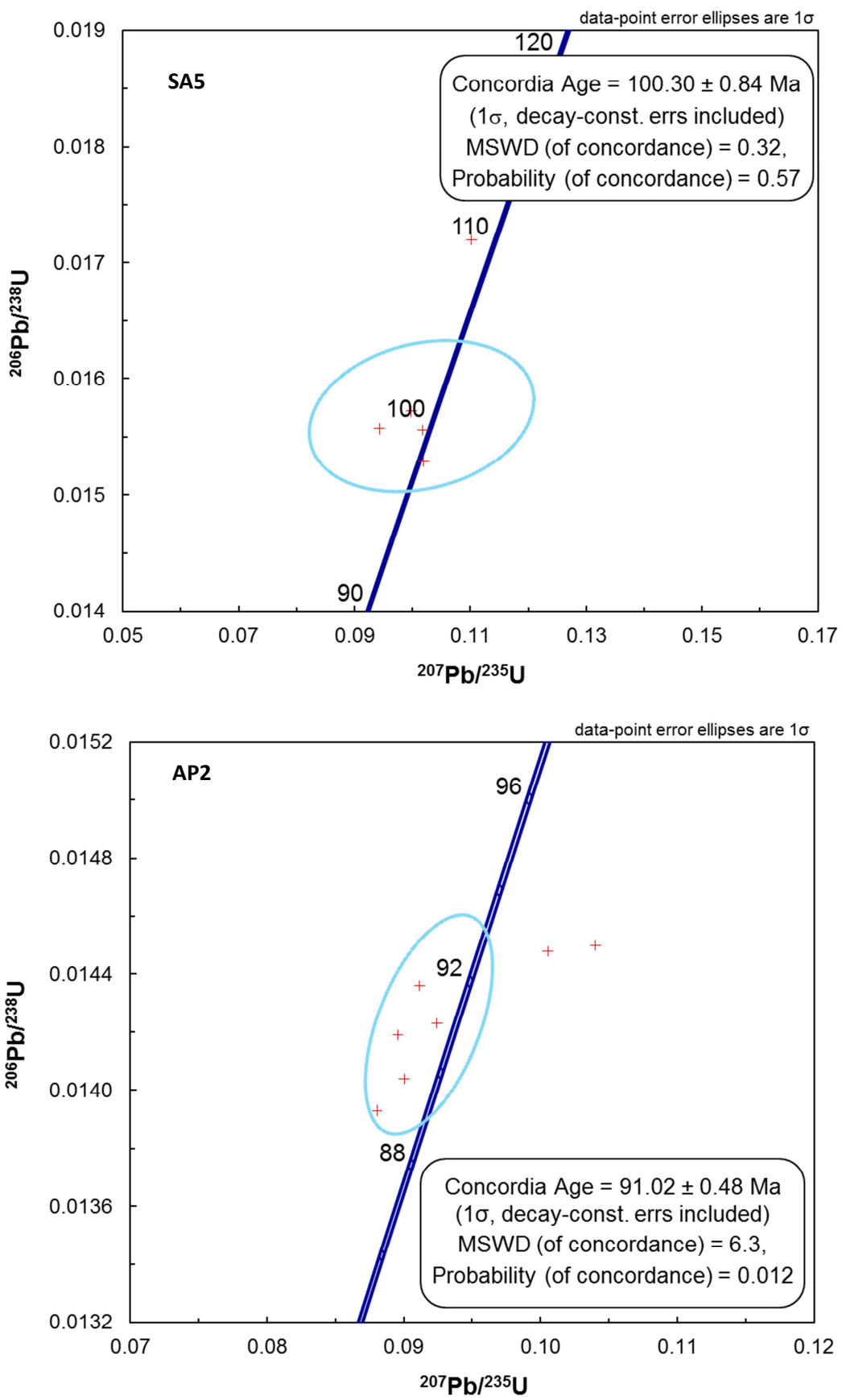


Figure DR2: t-T paths for AP1, AP2, AP3 and SA2-5. Path colours indicate good (purple) and acceptable (green) fits, based on comparison to measured AFT and AHe ages, and fission track lengths (Ketcham, 2005). Histograms show fission track length distributions for AP1 and AP2. Time axes for samples AP3 and SA2-5 are truncated because *t*-T histories for these are unconstrained prior to the early Miocene.

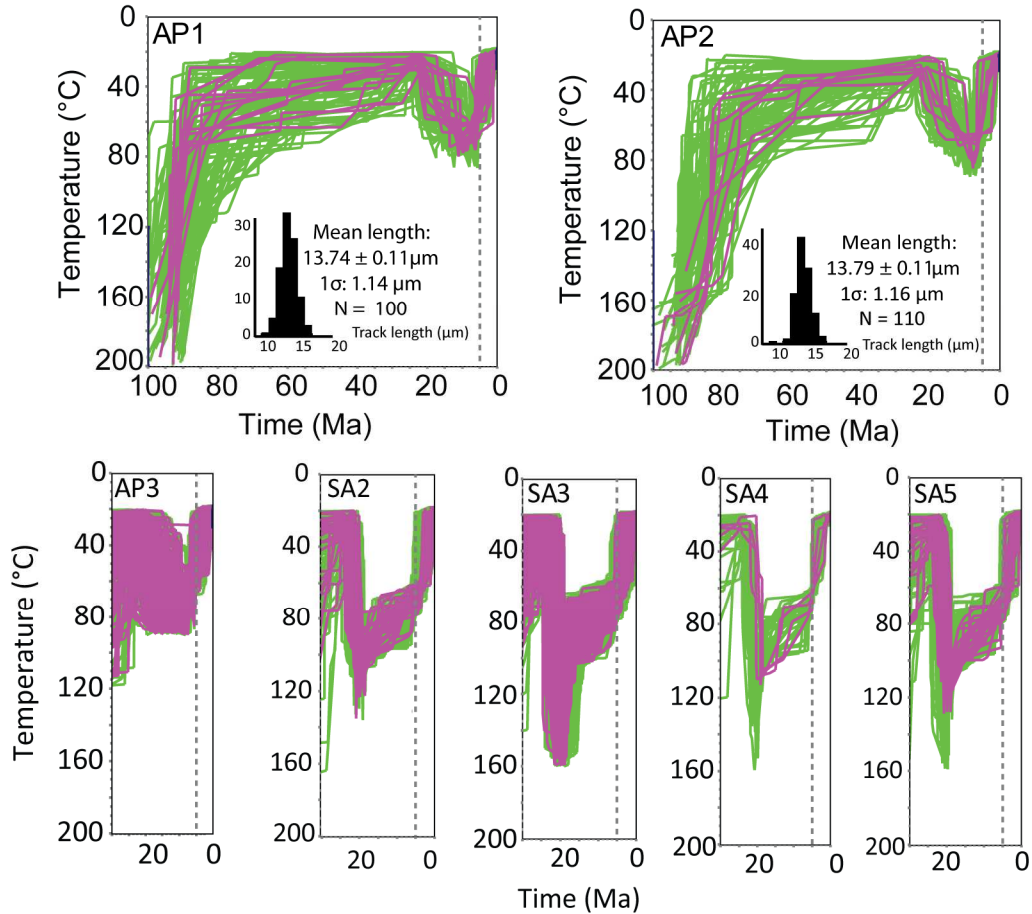


Figure DR3: Details of rift flank stratigraphy. $^{40}\text{Ar}/^{39}\text{Ar}$ ages are in Ma. Note that post-subduction lavas >5.6 Ma are components of mesa-summit relict landscape, while younger lavas also infill canyons. Background topography of the Loreto rift segment is from ASTER data.

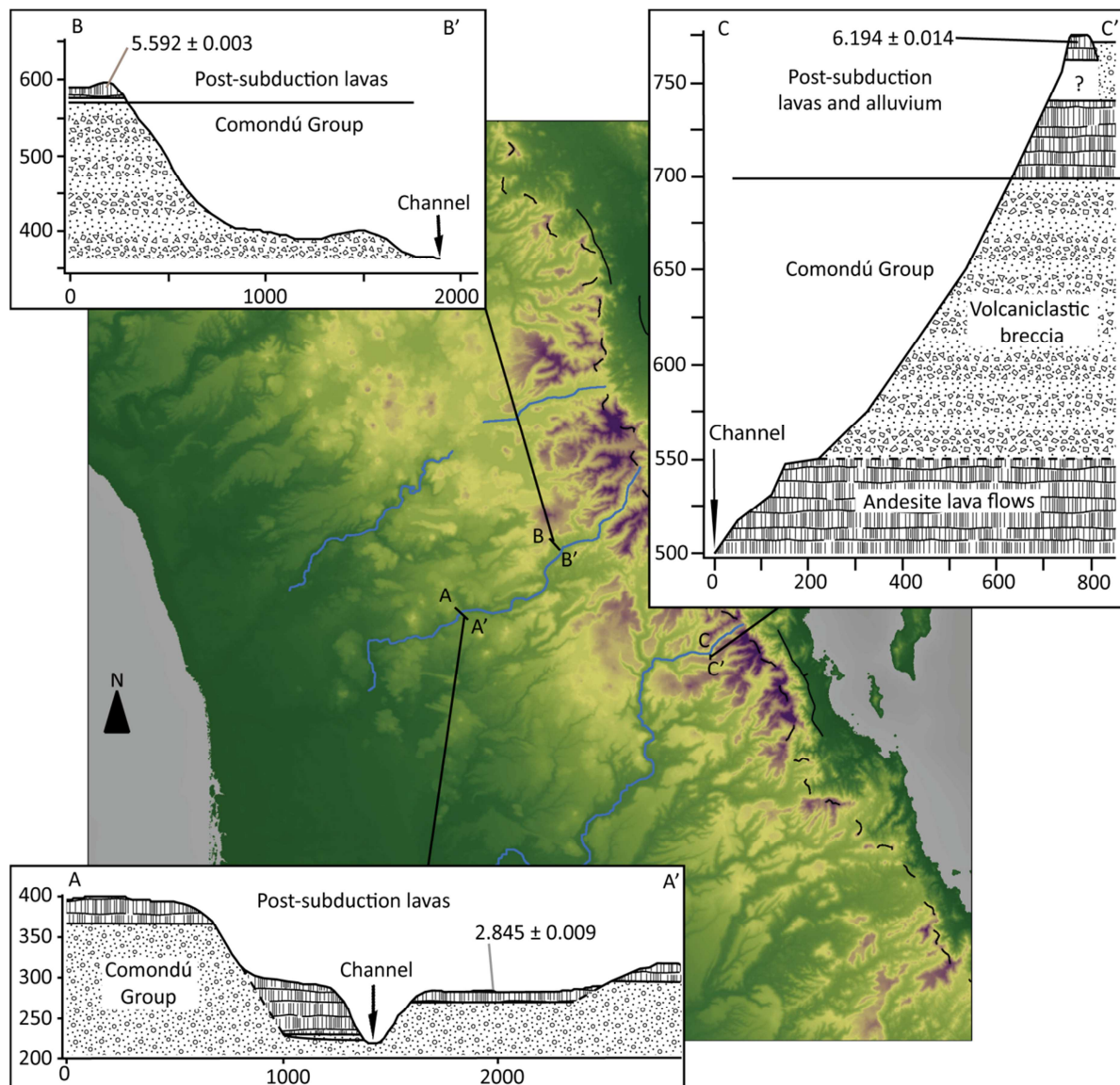


Figure DR4: Lithologies of clasts from relict surface alluvial cobbles atop interfluve mesas. Lithologies comprise Comondú andesite, pink/purple/grey, \pm <5% hornblende and plagioclase feldspar (1); post-subduction basaltic andesite (2); Comondú andesite dyke, grey, ~15 to 20 % euhedral hornblende (3); white pumice tuff with ~5% andesite lapilli (4); Comondú conglomerate (5). 101 clasts, all >5 cm in length, were identified at each location along a 3 m measure atop the alluvial surface. Background topography of the Loreto rift segment is from ASTER data.

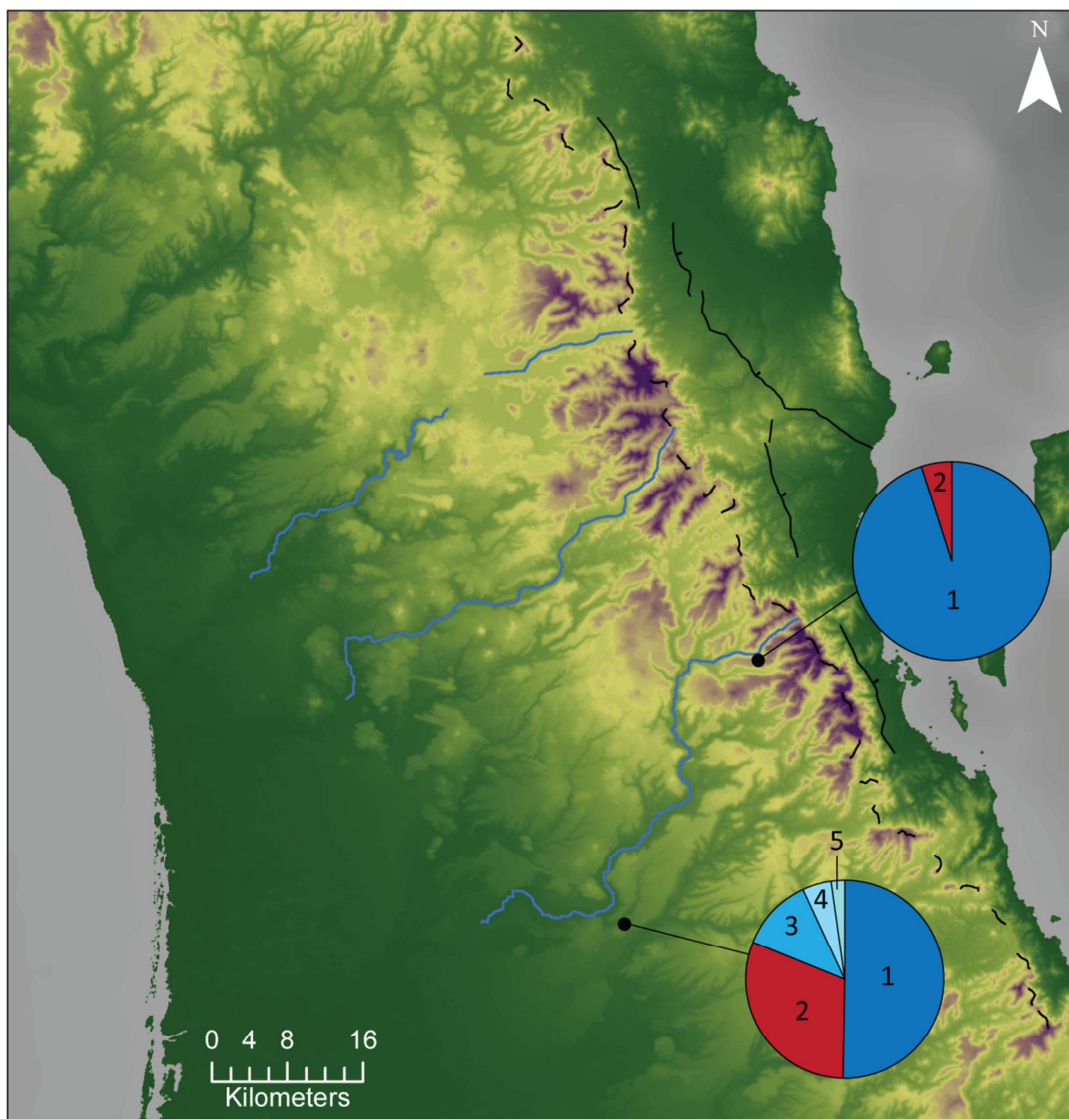


Figure DR5: The relict landscape. **A**, location. **B**, mesa-summit relict landscape, looking SW. Post-subduction lava outlined in red has been incised by San Javier canyon (out of frame, to right). $^{40}\text{Ar}/^{39}\text{Ar}$ age given in Ma. **C**, detail of alluvial cobbles exposed between lavas. Tape scale is 1 m.

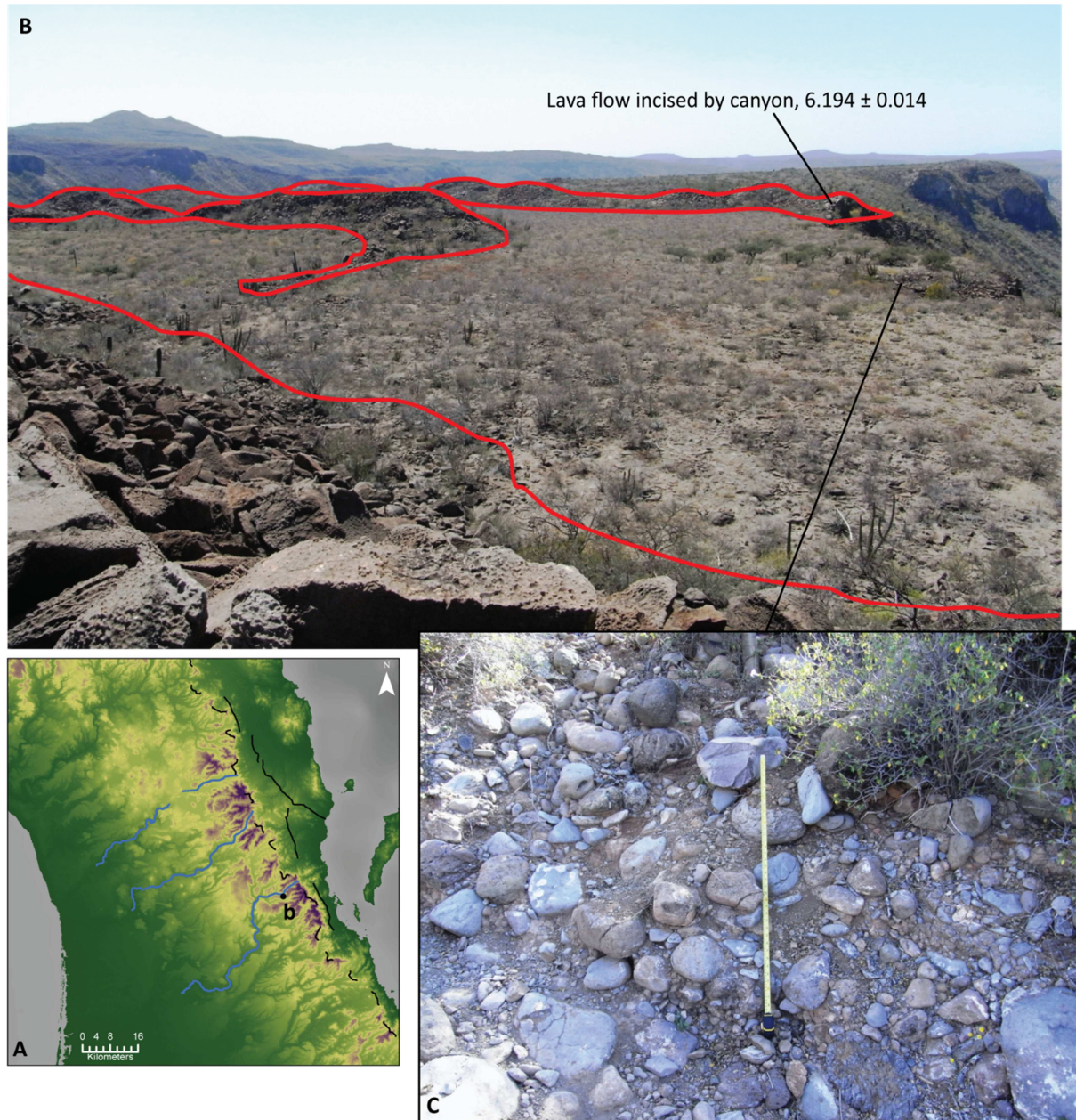


Figure DR6: A, location. B, image of ~3.2 Ma lava dam (outlined in red) in Comondú canyon, looking SW. Note lake in centre of image – the canyon upstream of the lava dam no longer drains to the Pacific. C, detail of lava dam in Comondú tributary canyon to south, looking SW. Geologist atop flow for scale.

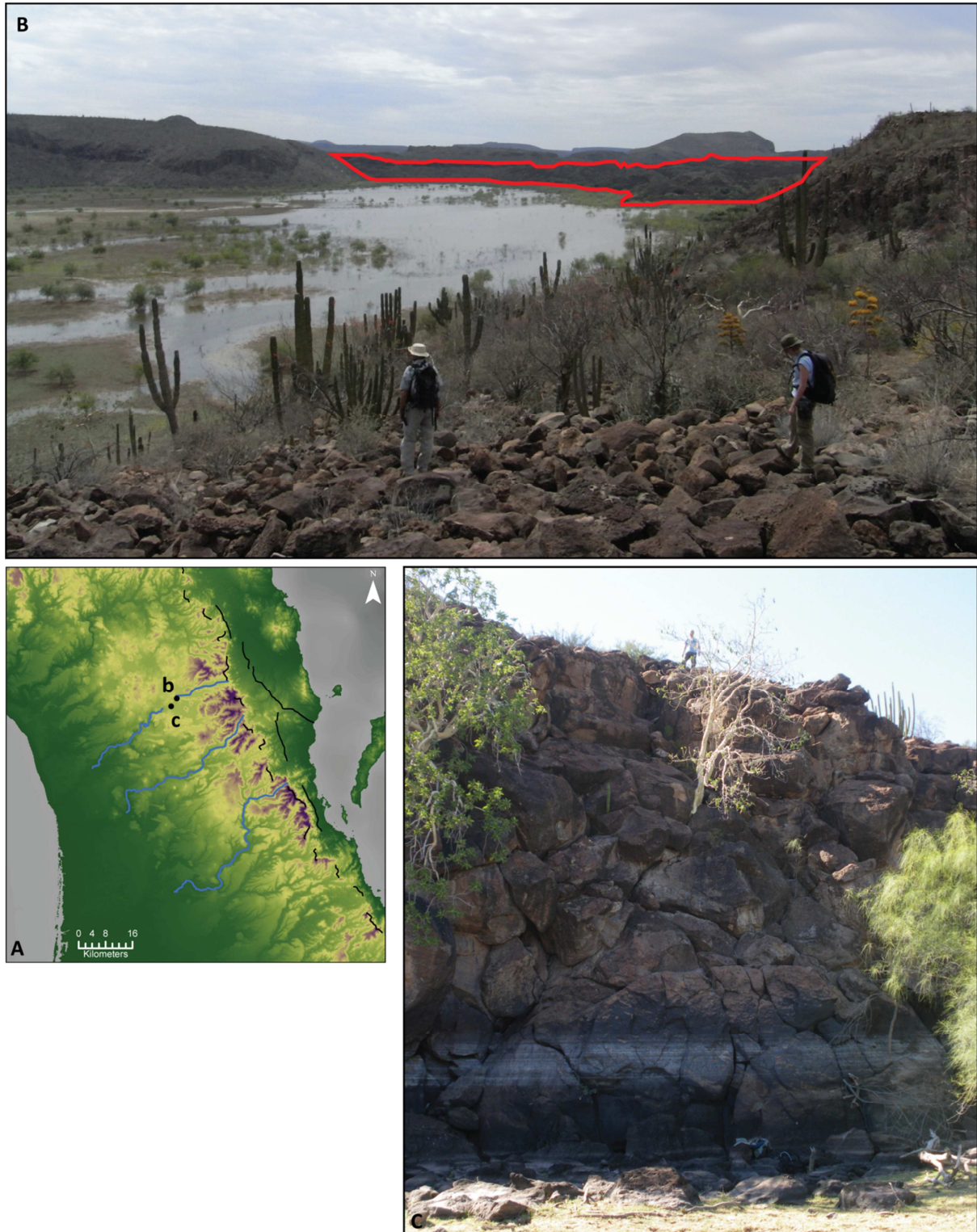
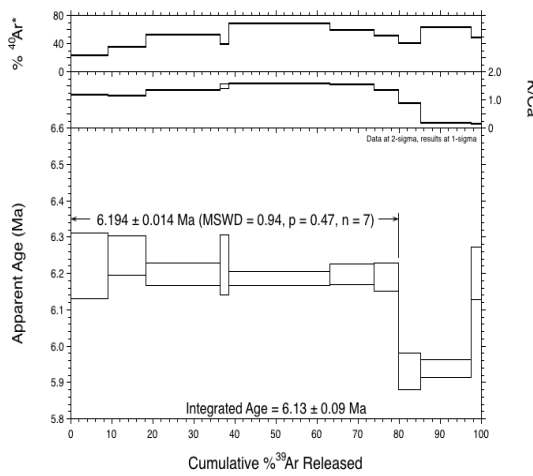
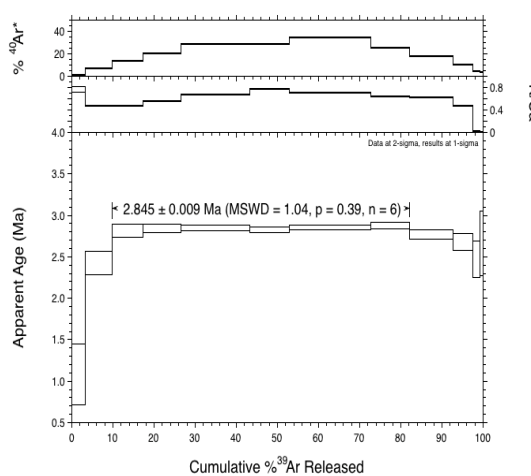


Figure DR7: $^{40}\text{Ar}/^{39}\text{Ar}$ step heating plots, showing plateau and integrated ages.

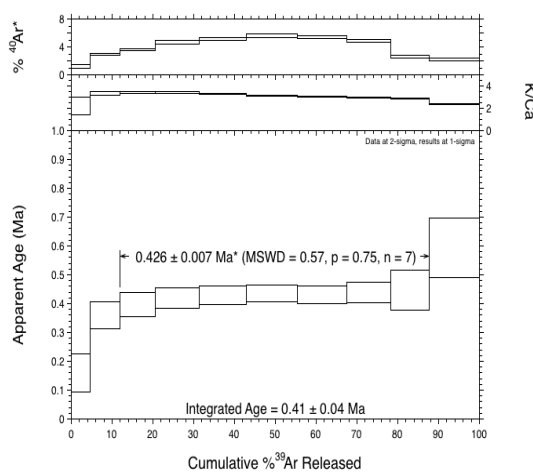
#27:



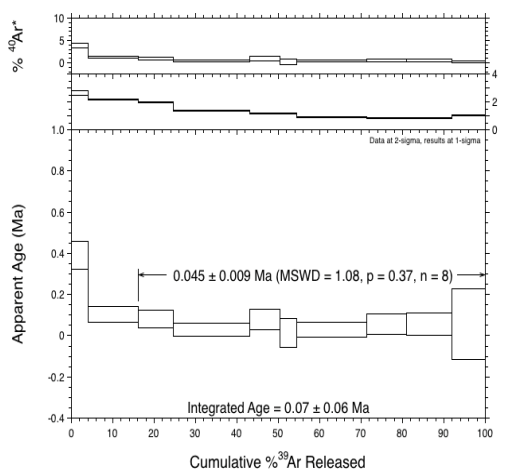
#31:



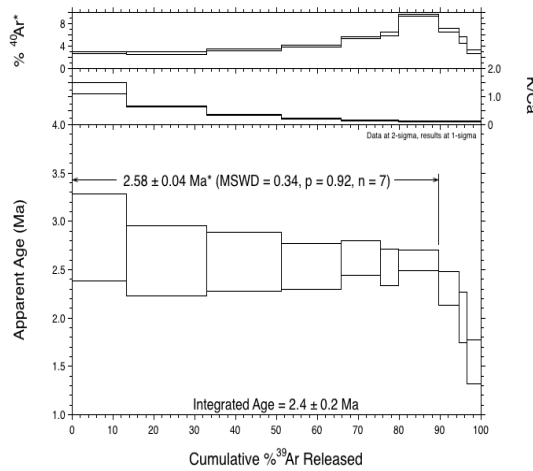
#40:



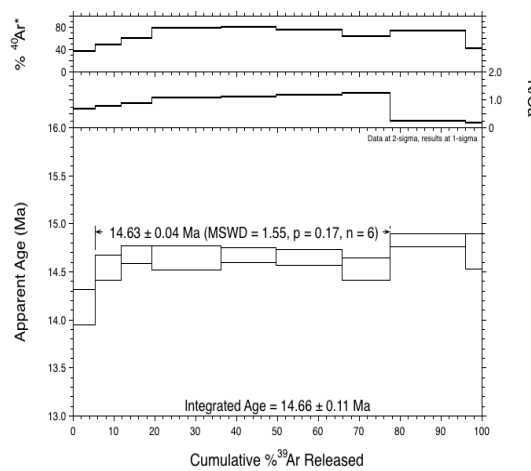
#44:



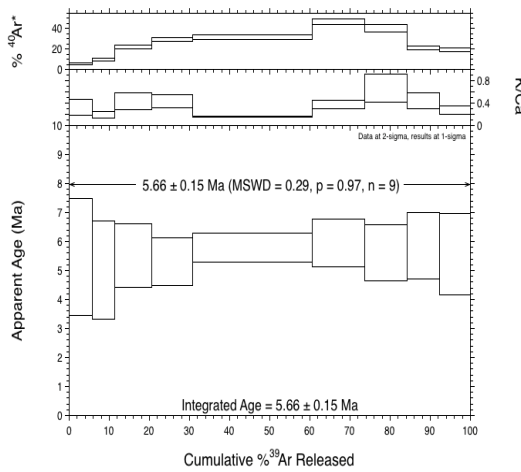
#47:



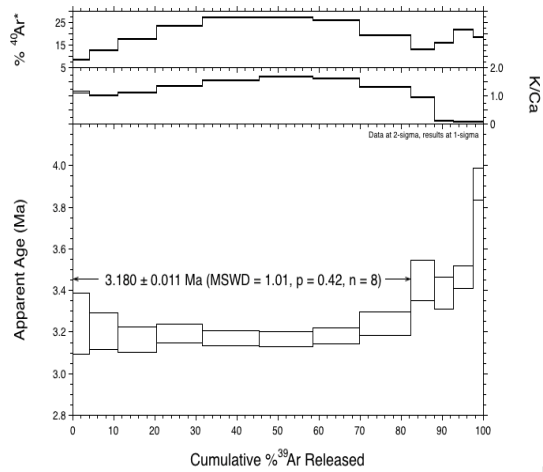
#48:



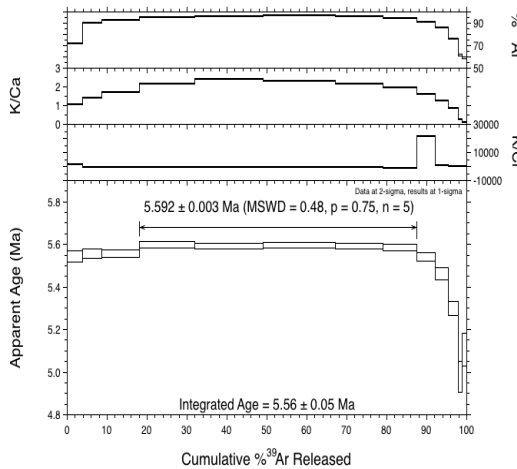
#52:



#F09:



#29:



#34:

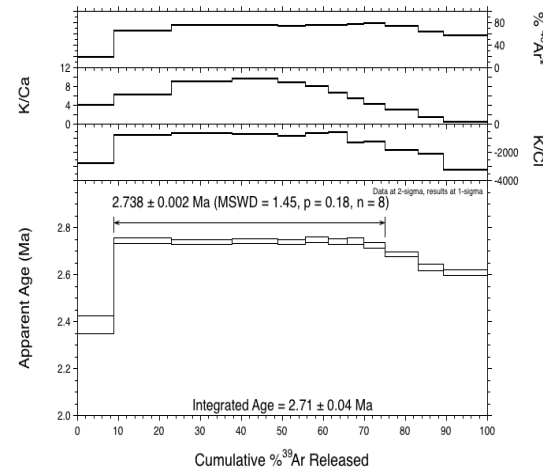
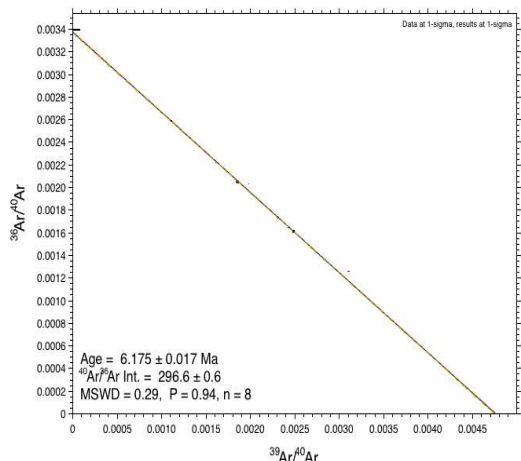
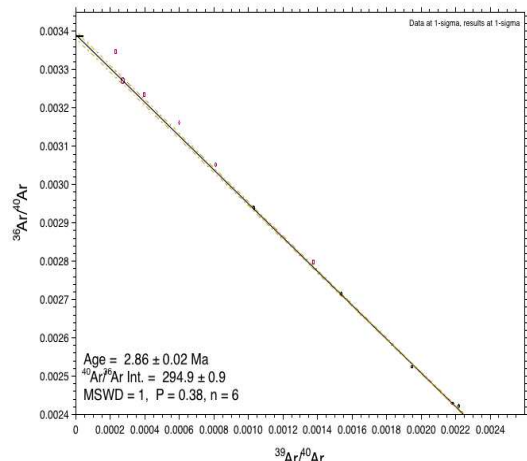


Figure DR8: $^{40}\text{Ar}/^{39}\text{Ar}$ inverse isochron plots.

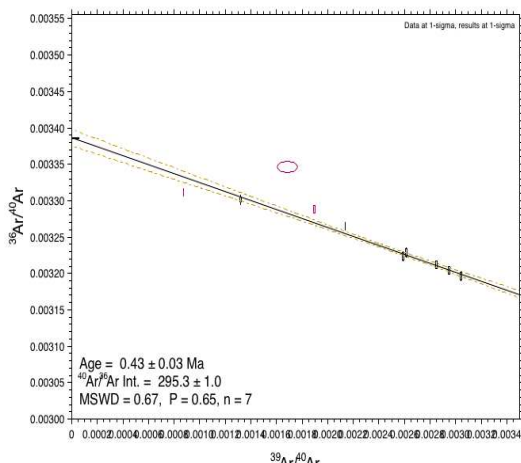
#27:



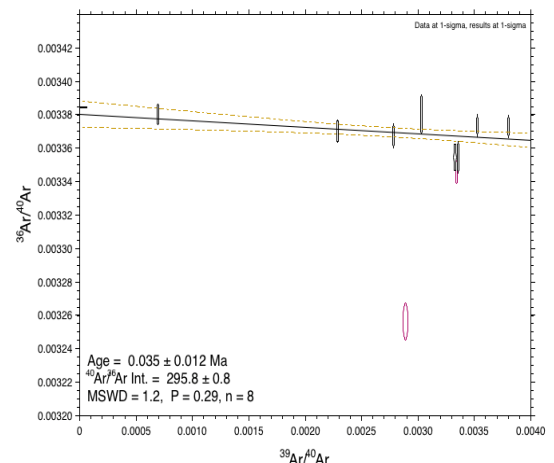
#31:



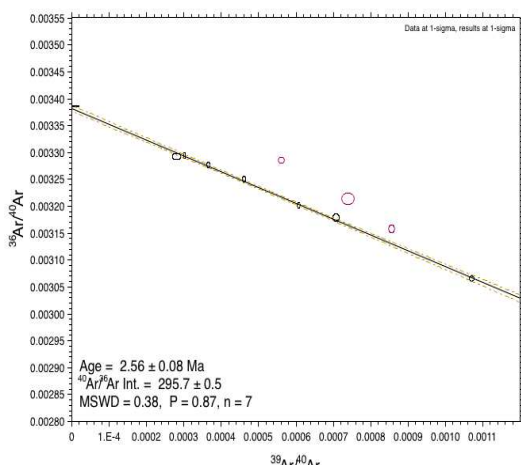
#40:



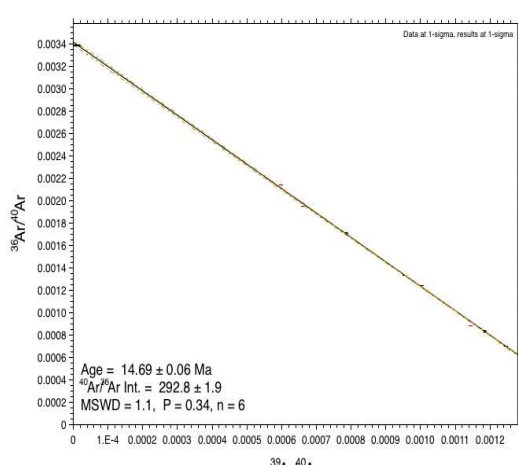
#44:



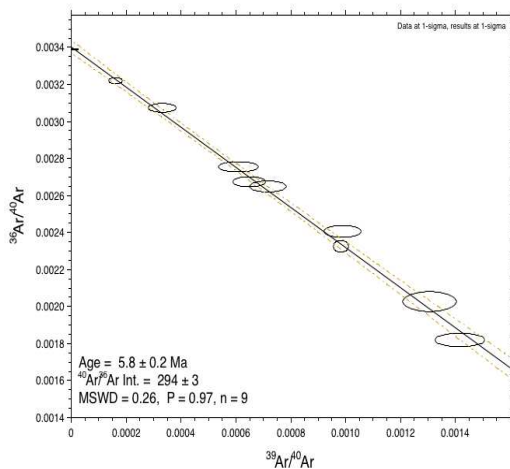
#47:



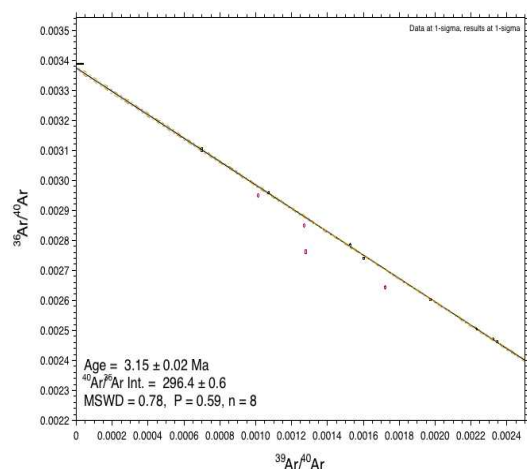
#48:



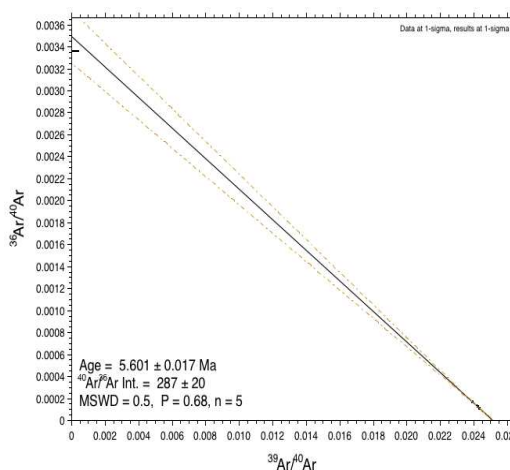
#52:



#F09:



#29:



#34:

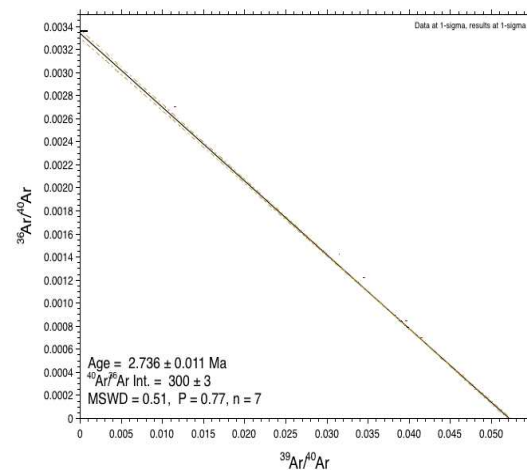


Figure DR9: Data used for flexure modelling. **A**, location of combined topographic/bathymetric profile obtained from GMRT (Ryan et al., 2009) data. **B**, topographic/bathymetric profile (blue) used to obtain unloading profile (red).

